C.I. Bajer, B. Dyniewicz. Virtual functions of the space-time finite element method in moving mass problems. Comp. and Struct., 79(3), 2009, pp. 213-223.

Virtual functions of the space-time finite element method in moving mass problems

Czesław I. Bajer and Bartłomiej Dyniewicz

Institute of Fundamental Technological Research, Polish Academy of Sciences, Świętokrzyska 21, 00-049 Warsaw, Poland.

Abstract

Classical time integration schemes fail in vibration analysis of complex problems with moving concentrated parameters. Moving mass problems and moving support problems belong to this group. Commercial systems of dynamic simulations do not support such an analysis. Moreover, the classical finite element method with the Newmark-type time integration method does not allow us to obtain convergent results at all. The reason lies in the impossibility of full mathematical consideration of the time integration stage and the analysis of inertial terms of a travelling mass. Both of them, unfortunately, are decoupled. In this paper we propose an efficient and exact numerical approach to the problem by using the space-time finite element method. We derive characteristic matrices of the discrete element of the string and the Bernoulli-Euler beam that carry the concentrated mass. We present four types of virtual functions in time and we apply two of them to the practical analysis. Displacements in time obtained numerically are compared with semi-analytical results. Almost perfect coincidence proves the efficiency of the approach.

Keywords: space-time finite element method, vibrations, virtual function, moving mass

1 Introduction

The paper deals with the numerical approach to the problem of structural vibrations under a travelling inertial load. Travelling non-inertial loads are unlikely to be solved by commercial codes. Such problems are not implemented in most of them. Inertial loads are not implemented in computer systems at all. Problems with travelling masses are of special interest in engineering practice. The influence of the mass attached locally to the structure cannot be neglected. We can only mention

here the coupling of the 500 kg mass of the train wheel with a rail or a track. A similar case occurs in problems concerning railway power collectors. The speed of the rail vehicle can reach the critical value. In such a case the wave response significantly differs from the response of massless systems.

In the paper we present an algorithm for the moving mass analysis in the case of unidimensional structures: a string or a bar and the Bernoulli-Euler beam. In the case of other types of structures the approach is identical. We derive and list the matrices explicitly. The resulting characteristic matrices can be directly applied to numerical algorithms. The principle of application of the space-time finite element method to the problem with inertial travelling load was presented by [1] who showed the way from the differential equation to the numerical scheme and the step-by-step formula by use of the space-time element method. The solution was limited to the simplest problem of string vibrations and to the use of the Dirac delta function as a virtual distribution of the velocity. The quality of the solution could, however, be improved by the application of modified virtual functions in the formulation. This paper will describe the solution of the problem with higher accuracy formulas and apply them to more complex structures – beams.

The classical finite element approach to the moving mass problems with the Newmark time integration method fails. The difficulty lies in the methodology of the solution of the variable coefficients differential equation with the classical time integration method. In this case the spatial discretisation is performed at a selected time point t_i. Vertical acceleration is expressed in the travelling point $x = vt$. The solution is obtained by introduction of the so-called Renaudot formula, which in fact is the chain-rule derivative of the vertical displacement. Thus the acceleration in the inertial term, for $x = vt$, results in three terms

$$\frac{\mathrm{d}^2 u(vt,t)}{\mathrm{d}t^2} = \left.\frac{\partial^2 u(x,t)}{\partial t^2}\right|_{x=vt} + 2v \left.\frac{\partial^2 u(x,t)}{\partial x \partial t}\right|_{x=vt} + v^2 \left.\frac{\partial^2 u(x,t)}{\partial x^2}\right|_{x=vt}, \tag{1}$$

interpreted as the vertical acceleration, the Coriolis acceleration and the centrifugal acceleration, respectively. The direct use of (1) in the differential equation governing the motion of the continuous structure results in wrong formulas, since this mathematical step is executed rather automatically, based on two separate mathematical stages: construction of the time integration scheme and contribution of the moving mass term based on (1). Then characteristic matrices, i.e. mass, damping, stiffness, etc., are established. They are related to time t_i and do not contribute properly to the influence of terms with variable coefficients.

A simple ad hoc mass splitting between neighbouring nodes (Figure 1) results in divergence as well. In some cases, especially in beams, numerical solutions are limited, but very inaccurate. In the case of string vibrations, governed by a purely hyperbolic differential equation, such a strategy results in divergent solutions. The ad hoc lumping can be applied in one particular case only: the mass must be replaced from node to node as a whole value. In practice, the mesh must be sized

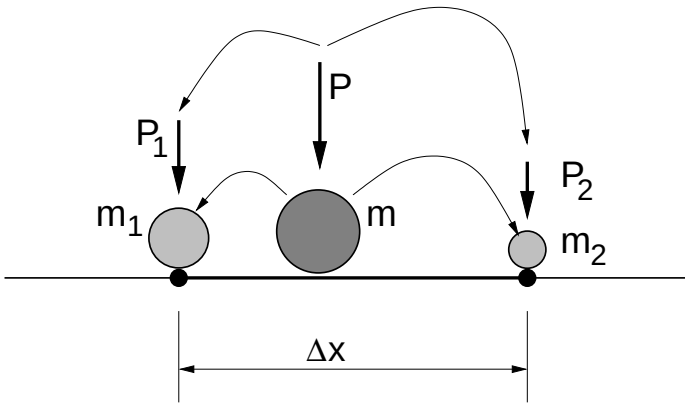

Figure 1: Ad hoc moving mass lumping in nodes.

in relation to the time step and mass velocity: $\Delta x = v\,\Delta t$. It makes the solutions useless. We are sure that classical time integration methods would result in correct formulas if they were preceded by a correctly performed analysis. Unfortunately, up till now the authors have not been successful.

Contrary to the classical approach, the space-time finite element method allows us to perform consequently the solution of the variable coefficient differential equation in time interval $[t_i, t_{i+1}]$. The time stepping formula is derived together with the analysis of the travelling mass vertical acceleration. This last feature requires a more complex mathematical analysis. The typical approach to the space-time element method with a Dirac delta virtual function allows us to derive characteristic matrices in the step-by-step procedure. In this case, however, the product of Dirac delta virtual function and the second Dirac delta function describing the concentrated moving mass must be integrated over space and time. Although the resulting time stepping scheme is unconditionally stable with respect to the time step, the accuracy for longer time steps can be insufficient. Below, we consider other virtual functions which result in relatively simple interpretation and ensure higher-order accuracy.

The space-time finite element approach differs from the classical finite element method. First of all, in a classical approach the spatial and temporal discretisation are carried on separately. The space domain of the structure is discretized, for example, by the finite element method, finite difference method, boundary element method, etc. Time integration is performed by a difference method. The Newmark method or a derivative method, i.e. the central difference scheme and trapezoidal rule, is usually applied at this stage. Well-known classical methods of integration of the differential equations like Runge-Kutta methods, Adams methods and others can also be placed in this group. A classical approach to the vibration analysis of the structure can shortly be written by relations which describe the global (i.e. both in space and in time) interpolation of fundamental

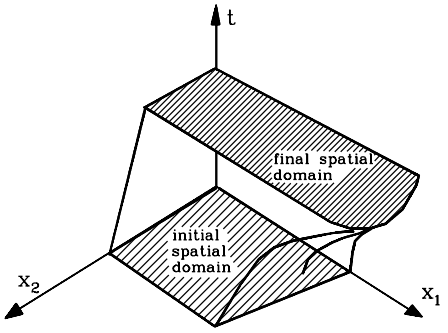

Figure 2: Space-time subdomain.

quantities:

$$q(\mathbf{x},t) = \mathbf{N}(\mathbf{x})\,\mathbf{T}(t)\,\mathbf{q}_e \quad . \tag{2}$$

$\mathbf{N}(\mathbf{x})$ is the interpolation formula applied to space, for example, shape functions in the FEM, and $\mathbf{T}(t)$ is a time interpolation of the nodal quantity $\mathbf{q}_e = [\mathbf{q}_i, \mathbf{q}_{i+1}]^T$ in two while limiting the time interval $[t_i, t_{i+1}]$. Let us examine the uncoupling of both functions. The space-time finite element approach is described by the following interpolation:

$$q(\mathbf{x},t) = \mathbf{N}(\mathbf{x},t)\,\mathbf{q}_e \quad . \tag{3}$$

$\mathbf{N}(\mathbf{x},t)$ is the matrix interpolation function defined in a space-time subdomain (Figure 2). We emphasise here that the form of Eqn. (3) is more general than (2) and the classical finite element approach can be considered as a particular case of the space-time element method. In the space-time approach a non-stationary discretisation can also be used. In the case of a stationary mesh and in problems without damping, one can write a pass from one approach to another. Characteristic matrices, however, differ. In a general case both approaches differ. This also occurs in the case of spatial elements carrying the travelling mass. Here the second fundamental difference must be emphasised: the finite element approach uses the difference schemes for time integration while the space-time approach uses the integral formulas in formulation of the resulting time stepping schemes.

We have said that the string solution diverges even at low velocity range and with small ratio of the moving mass to the span mass. In Figure 3 the moving mass to string mass ratio was equal to 0.1 and the mass velocity was below 0.2 of the wave speed in the string. In practice these values are relatively low. Real problems require both parameters to be even greater than one. We should be able to simulate the following technical problems: vibrations of railway tracks, vehicle passing over bridges, pantograph collectors in railways, magnetic railways, guideways in robotic technology, gun barrel, airfield plates, etc. In the case of a beam or a plate, numerical solutions are usually limited, because of parabolic terms in the differential equation. They are, however, highly

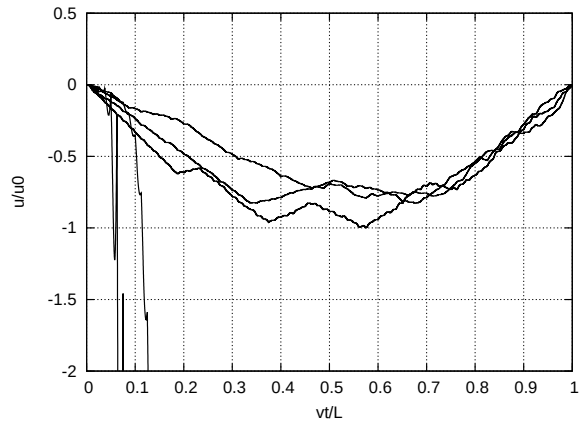

Figure 3: Divergence of the existing numerical solutions.

inaccurate. Several papers deal with the discrete analysis of the moving mass problem [2, 3, 4]. Unfortunately, the authors do not present numerical results obtained for the inertial load. A simple massless force or oscillator is used in theirdemonstration, or theoretical and experimental results are only compared. All of the so-called mass forces finally are replaced by massless loads. What is more, the analytical derivations do not consider correctly the fundamental inertial term

$$\delta(x - vt)\, m\, \frac{\partial^2 u(vt,t)}{\partial t^2}$$

in the solution of the differential equation [5, 6] (compare with [7, 8]). Here u is the string deflection and m is the mass moving with the constant velocity v.

The problem of a string vibration is not trivial. First of all we must emphasise the discontinuity of the mass particle trajectory moving on the string, at the end support. This phenomenon was reported in the literature for the first time in [7, 8] and was mathematically proved in the case of a massless string. In the case of the inertial string, the discontinuous motion of the mass was demonstrated. We can observe but we cannot prove the discontinuity of the string at the end support. We can, however, expect high gradients of the solution and that they will be accompanied by problems with discrete solutions.

The only efficient discrete solution of the problem with moving mass being in direct contact with a string or a beam can so far be performed only with the use of the space-time finite element method. Fundamentals of this approach are discussed in detail in numerous references. The displacement formulation is presented in [9, 10]. The stationary and non-stationary discretisation of the time space, stability problems and applications can be found in [11, 12]. The velocity formulation developed in this paper is presented in [13, 14]. Below we describe the method briefly. In further sections, the influence of virtual functions on the accuracy of the solution of the moving mass problem will be discussed. The space-time finite element characteristic matrices of the element

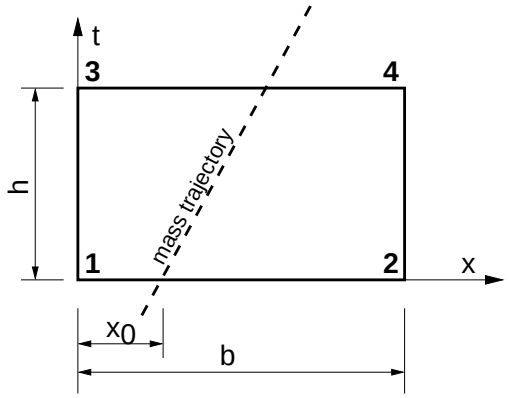

Figure 4: Mass trajectory in time-space.

carrying the mass particle will be given. The accuracy of displacements in the middle of the span and under the mass will be demonstrated in comparison with semi-analytical results.

2 Basics of the space-time finite element approach formulated in velocities

The reader is referred here at least to [13, 14]. Below, the main idea of the formulation in the case of the string will be given in brief.

The space-time approach requires the description of the phenomenon in the space-time interval. We consider not only states at times t_i and t_{i+1} that limit the time interval, but also its interior. We can assume various functions of the virtual distribution of the phenomenon. Moreover, we can incorporate a special function that describes the action of the particular factor in space and in time. In our case the mass moving along a given trajectory in time-space is the point of interest (Figure 4).

We consider the well-known equation of the string vibration

$$-N\,\frac{\partial^2 u(x,t)}{\partial x^2}\;+\;\rho A\,\frac{\partial^2 u(x,t)}{\partial t^2}\;=\;\delta(x-vt)\,P\;-\;\delta(x-vt)\,m\,\frac{\partial^2 u(vt,t)}{\partial t^2} \tag{4}$$

in the space-time domain $\Omega=\{(x,t)\colon 0\le x\le b,\;\;0\le t\le h\}$. b is the length of the spatial finite element and h is the time step. In the next part for simplicity we consider the uniform equation. The equation of the virtual power is obtained by multiplying the motion equation by the virtual velocity $v^*(x,t)$. For simplicity we consider here a uniform differential equation. The total virtual power in Ω is given as the integral

$$\int_0^h\int_0^b v^*(x,t)\,\left(\rho A\frac{\partial^2 u}{\partial t^2}-N\frac{\partial^2 u}{\partial x^2}-\eta\frac{\partial u}{\partial t}\right)\mathrm{d}x\,\mathrm{d}t=0\;. \tag{5}$$

Here η denotes internal damping coefficient. The displacement $u(x,t)$ and the derivative $\partial u/\partial x$ are expressed in terms of a velocity $v(x,t)$:

$$u(x,t) = u_0(x) + \int_0^t v(x,t)\mathrm{d}t \ , \quad \frac{\partial u(x,t)}{\partial x} = \varepsilon_0(x) + \int_0^t v(x,t)\mathrm{d}t \ . \tag{6}$$

ε_0 is a strain at the beginning of the time step. Node numbering in the space-time element is presented in Figure 4. Integrating (5) by parts with respect to x results in the equation

$$\rho A \iint_\Omega v^* \frac{\partial v}{\partial t}\,\mathrm{d}\Omega + N \iint_\Omega \frac{\partial v^*}{\partial x}\frac{\partial u}{\partial x}\,\mathrm{d}\Omega + \iint_\Omega \frac{\partial v^*}{\partial x}\varepsilon_0\,\mathrm{d}\Omega - \eta \iint_\Omega v^* v\,\mathrm{d}\Omega = 0 \ . \tag{7}$$

We assume a linear variation of the velocity $v = \partial u/\partial t$ with x and t:

$$v(x,t) = \sum_{i=1}^{4} N_i(x,t)\, v_i \ . \tag{8}$$

In the domain Ω the shape function $\mathbf{N} = [N_1, \ldots, N_4]$ has the form:

$$\mathbf{N} = \left[\frac{1}{bh}(x-b)(t-h) \ , \quad -\frac{1}{bh}\,x(t-h) \ , \quad -\frac{1}{bh}(x-b)t \ , \quad \frac{1}{bh}\,x\,t\right] \ . \tag{9}$$

Displacements are computed from the velocity equation by integration

$$u(x,t) = u(x,0) + \int_0^t (N_1 v_1 + \ldots + N_4 v_4)\,\mathrm{d}t = u(x,0) + \int_0^t \mathbf{N}^*\,\mathrm{d}t\,\mathbf{v} \ . \tag{10}$$

The derivative $\partial u/\partial x$ can also be computed from (10).

The proper choice of virtual functions v^* is a fundamental question of the space-time approach. Different functions result in solution schemes of different properties: accuracy and stability. We propose a simple form with distribution δ in $t = \alpha h$ (Figure 5a).

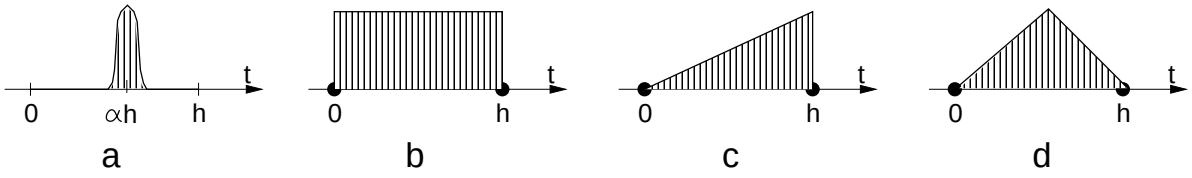

Figure 5: Virtual functions: a – Dirac delta shape, b – hat shape, c – triangle shape, d – roof shape.

$$v^*(x,t) = \delta(t-\alpha h)\left[(1-\frac{x}{b})v_3 + \frac{x}{b}\,v_4\right] \ . \tag{11}$$

Required derivatives of virtual v^* and real v functions can be determined from (8) and (11)

$$\frac{\partial v}{\partial t} = \frac{x}{bh}(v_1 - v_2 - v_3 + v_4) + \frac{1}{h}(-v_1 + v_3) \ , \tag{12}$$

$$\frac{\partial v^*}{\partial x} = \frac{1}{b}(-v_3 + v_4) \ . \tag{13}$$

We note that the Dirac δ term in the integrand reduces the integration in Ω to the integration over $0 \le x \le b$. Finally, the Eqn. (7) can be written in the following matrix form:

$$\left\{ \rho A \int_0^b \begin{bmatrix} -\left(\frac{x}{b}-1\right) \\ \frac{x}{b} \end{bmatrix} \left[\tfrac{x}{bh}-\tfrac{1}{h},\ -\tfrac{x}{bh},\ -\tfrac{x}{bh}+\tfrac{1}{h},\ \tfrac{x}{bh}\right] \mathrm{d}x \right.$$
$$+N \int_0^b \begin{bmatrix} -\frac{1}{b} \\ \frac{1}{b} \end{bmatrix} \left[\tfrac{t^2}{2bh}-\tfrac{t}{b},\ -\tfrac{t^2}{2bh}+\tfrac{t}{b},\ -\tfrac{t^2}{2bh},\ \tfrac{t^2}{2bh}\right] \mathrm{d}x\Big|_{t=\alpha h} + N \int_0^b \begin{bmatrix} -\frac{1}{b} \\ \frac{1}{b} \end{bmatrix} \varepsilon_0 \, \mathrm{d}x \qquad (14)$$
$$\left. - \eta \int_0^b \begin{bmatrix} -(\frac{x}{b}-1) \\ \frac{x}{b} \end{bmatrix} \left[\tfrac{(x-b)(t-h)}{bh},\ -\tfrac{x(t-h)}{bh},\ -\tfrac{(x-b)t}{bh},\ \tfrac{xt}{bh}\right] \mathrm{d}x\Big|_{t=\alpha h} \right\} \begin{Bmatrix} v_1 \\ \vdots \\ v_4 \end{Bmatrix} = \mathbf{0} \ .$$

The resulting matrices are listed below:

$$\mathbf{M} = \frac{\rho b}{h} \left[\begin{array}{cc|cc} -\frac{1}{3} & -\frac{1}{6} & \frac{1}{3} & \frac{1}{6} \\ -\frac{1}{6} & -\frac{1}{3} & \frac{1}{6} & \frac{1}{3} \end{array}\right] = \frac{1}{h} \left[-\mathbf{M}_s \mid \mathbf{M}_s\right] \ , \qquad (15)$$

$$\mathbf{K} = \frac{Nh}{b} \left[\begin{array}{cc|cc} \alpha(1-\frac{\alpha}{2}) & -\alpha(1-\frac{\alpha}{2}) & \frac{\alpha^2}{2} & -\frac{\alpha^2}{2} \\ -\alpha(1-\frac{\alpha}{2}) & \alpha(1-\frac{\alpha}{2}) & -\frac{\alpha^2}{2} & \frac{\alpha^2}{2} \end{array}\right] =$$
$$= h \left[\alpha(1-\frac{\alpha}{2})\mathbf{K}_s \mid \frac{\alpha^2}{2}\mathbf{K}_s\right] \ , \qquad (16)$$

$$\mathbf{C} = \eta b \left[\begin{array}{cc|cc} \frac{1-\alpha}{3} & \frac{1-\alpha}{6} & \frac{\alpha}{3} & \frac{\alpha}{6} \\ \frac{1-\alpha}{6} & \frac{1-\alpha}{3} & \frac{\alpha}{6} & \frac{\alpha}{3} \end{array}\right] = \left[(1-\alpha)\mathbf{C}_s \mid \alpha\mathbf{C}_s\right] \ . \qquad (17)$$

$\mathbf{M}$, $\mathbf{K}$, and $\mathbf{C}$ are the space-time inertia, stiffness and viscous damping matrices, respectively. We note that they are composed of two square matrices, each of a dimension equal to the number of degrees of freedom in a spatial finite element. Matrices $\mathbf{M_s}$, $\mathbf{K_s}$, and $\mathbf{C_s}$ have the same or similar forms to respective matrices derived traditionally from the classical finite element approach. The final form of the motion equation establishes the force equilibrium on the edge of the element domain Ω. Vector $\mathbf{v}$ contains nodal velocities $\mathbf{v}_i$ at the initial time $t = t_i$ and $\mathbf{v}_{i+1}$ at the final time $t = t_i + h$.

$$(\mathbf{M}+\mathbf{C}+\mathbf{K}) \begin{Bmatrix} \mathbf{v}_i \\ \mathbf{v}_{i+1} \end{Bmatrix} + \mathbf{e}_i = \mathbf{F}_i \quad \text{or} \quad \mathbf{K}^* \, \mathbf{v} + \mathbf{e}_i = \mathbf{F}_i \quad \text{or} \quad [\mathbf{K}_L^* | \mathbf{K}_R^*] \begin{Bmatrix} \mathbf{v}_i \\ \mathbf{v}_{i+1} \end{Bmatrix} + \mathbf{e}_i = \mathbf{F}_i \ . \qquad (18)$$

We add here (previously neglected for simplicity) the vector of external forces placed in nodes $\mathbf{F}_i$. $\mathbf{e}_i$ is a vector of nodal forces at the beginning of the time interval. It can be computed as a product of a square matrix $\mathbf{E}$ (in the case of the simplest problems it is the stiffness matrix derived from the finite element method) and the displacement vector $\mathbf{q}_i$ at t_i:

$$\mathbf{e}_i = \mathbf{E} \, \mathbf{q}_i \ . \qquad (19)$$

The velocity vector $\mathbf{v}_{i+1}$ is the only unknown vector in the above step-by-step equation. The final solution is described by the scheme

$$\mathbf{K}_R^* \ \mathbf{v}_{i+1} = \mathbf{F}_{i+1} - \mathbf{e}_i - \mathbf{K}_L^* \ \mathbf{v}_i \ . \tag{20}$$

Finally we must compute displacements $\mathbf{q}_{i+1}$. We use the formula

$$\mathbf{q}_{i+1} = \mathbf{q}_i + h[\beta \, \mathbf{v}_i + (1-\beta) \, \mathbf{v}_{i+1}] \ . \tag{21}$$

The stability analysis results in $\beta = 1 - \alpha$ for the Dirac delta virtual time functions.

3 Virtual shape functions in time

The method is identical to the analysis with the virtual function in the previous case (11). Let us consider the properties of virtual functions in other forms. The accuracy and the stability of the solution differ in each case. The question of the accuracy is important, especially in our case of the mass moving across the space-time subdomain. Below we will give stiffness and inertia matrices in the case of a bar in axial vibrations, derived with different virtual functions. We will also estimate the approximation error.

3.1 Global equilibrium (hat function)

We claim the global equilibrium in the interval $[0, h]$. We assume the constant value function (for example, equal to one) in the time interval (Figure 5b)

$$v^*(x,t) = (1 - \frac{x}{b}) \, v_3 + \frac{x}{b} \, v_4 \ . \tag{22}$$

Resulting stiffness and inertia matrices have the form

$$\mathbf{K} = \frac{EAh}{b} \left[\begin{array}{cc|cc} \frac{1}{3} & -\frac{1}{3} & \frac{1}{6} & -\frac{1}{6} \\ -\frac{1}{3} & \frac{1}{3} & -\frac{1}{6} & \frac{1}{6} \end{array} \right] \ , \tag{23}$$

$$\mathbf{M} = \frac{\rho Ab}{h} \left[\begin{array}{cc|cc} -\frac{1}{3} & -\frac{1}{6} & \frac{1}{3} & \frac{1}{6} \\ -\frac{1}{6} & -\frac{1}{3} & \frac{1}{6} & \frac{1}{3} \end{array} \right] \ . \tag{24}$$

Displacements in time t_{i+1} are computed from the average velocity $\mathbf{q}_{i+1} = \mathbf{q}_i + h \, [\beta \mathbf{v}_i + (1-\beta)\mathbf{v}_{i+1}]$. We obtain the stable solution in the wider range of the parameter β for $1/2 \leq \beta \leq 1$.

We expand the velocity and displacements into the Taylor series:

$$\begin{aligned} v_{i+1} &= \left(1 - \frac{1}{2}\omega^2 h^2 + \mathcal{O}(h^4)\right) v_i + \left(-\omega^2 h + \frac{1}{6}\omega^4 h^3 + \mathcal{O}(h^5)\right) u_i \ , \\ u_{i+1} &= \left(h - \frac{1}{2}\omega^2 h^3 (1-\beta) + \mathcal{O}(h^5)\right) v_i + \left(1 - \omega^2 h^2 (1-\beta) + \mathcal{O}(h^4)\right) u_i \ . \end{aligned} \tag{25}$$

We estimate the error of the velocity ϵ_v

$$\epsilon_v = \mathcal{O}(h^4)\, v_i + \mathcal{O}(h^5)\, u_i \tag{26}$$

and the error of the displacements ϵ_u

$$\epsilon_u = \left[\omega^2 h^3 \left(\frac{1}{3} - \frac{1}{2}\beta\right) + \mathcal{O}(h^5)\right] v_i + \left[\omega^2 h^2 \left(\frac{1}{2} - \beta\right) + \mathcal{O}(h^4)\right] u_i. \tag{27}$$

$\beta = 1/2$ results in the error proportional to $1/12\ h^3\omega^2$. This is the best choice for β. The solution scheme is unconditionally stable and exhibits the smallest error in comparison with other virtual functions.

3.2 Triangular function

We assume triangular distribution of the virtual function in time interval $[0, h]$ (Figure 5c)

$$v^*(x,t) = (1 - \frac{x}{b})\frac{t}{h}\, v_3 + \frac{x}{b}\frac{t}{h}\, v_4\ . \tag{28}$$

The stiffness and inertia matrices have the following coefficients:

$$\mathbf{K} = \frac{EAh}{b} \left[\begin{array}{cc|cc} \frac{5}{24} & -\frac{5}{24} & \frac{1}{8} & -\frac{1}{8} \\ -\frac{5}{24} & \frac{5}{24} & -\frac{1}{8} & \frac{1}{8} \end{array}\right] \ , \tag{29}$$

$$\mathbf{M} = \frac{\rho Ab}{h} \left[\begin{array}{cc|cc} -\frac{1}{6} & -\frac{1}{12} & \frac{1}{6} & \frac{1}{12} \\ -\frac{1}{12} & -\frac{1}{6} & \frac{1}{12} & \frac{1}{6} \end{array}\right] \ . \tag{30}$$

The stability criterion results in the parameter $2/3 \leq \beta \leq 1$.

3.3 Roof function

The roof virtual shape function in time is composed of two triangles, as presented in Figure 5d:

$$v^*(x,t) = \begin{cases} (1 - \frac{x}{b})\frac{2t}{h}\, v_3 + \frac{x}{b}\frac{2t}{h}\, v_4, & \text{with } \ 0 \leq t \leq t/2 \\ (1 - \frac{x}{b})(-\frac{2t}{h} + 2)\, v_3 + \frac{x}{b}(-\frac{2t}{h} + 2)\, v_4 & \text{with } \ t/2 < t \leq h \end{cases} \ . \tag{31}$$

Stiffness and mass matrices are similar to those in the previous cases

$$\mathbf{K} = \frac{EAh}{b} \left[\begin{array}{cc|cc} \frac{17}{96} & -\frac{17}{96} & \frac{7}{96} & -\frac{7}{96} \\ -\frac{17}{96} & \frac{17}{96} & -\frac{7}{96} & \frac{7}{96} \end{array}\right] \ , \tag{32}$$

$$\mathbf{M} = \frac{\rho Ab}{h} \left[\begin{array}{cc|cc} -\frac{1}{6} & -\frac{1}{12} & \frac{1}{6} & \frac{1}{12} \\ -\frac{1}{12} & -\frac{1}{6} & \frac{1}{12} & \frac{1}{6} \end{array}\right] \ . \tag{33}$$

We apply the stability criterion to determine the range of validity of the parameter β. It is $3/4 \leq \beta \leq 1$.

3.4 Dirac delta function (point equilibrium)

The distribution of the virtual function in a form of delta Dirac function was described in Section 2. Below we analyse the processes described by Eqns. (18, 21). The expansion of the velocity and displacements into the Taylor series allows us to determine the error in comparison with the expansion of sin and cos function, assumed to be the theoretical solutions of the problem

$$\begin{aligned} v_{i+1} &= \left(1-\alpha\omega^2h^2+\frac{1}{2}\alpha^3\omega^4h^4+\mathcal{O}(h^6)\right)v_i+\left(-\omega^2h+\frac{1}{2}\alpha^2\omega^4h^3+\mathcal{O}(h^5)\right)u_i \ , \\ u_{i+1} &= \left(h-\omega^2h^3\alpha(1-\alpha)+\mathcal{O}(h^5)\right)v_i+\left(1-\omega^2h^2\alpha+\frac{1}{2}\omega^4h^4\alpha^3+\mathcal{O}(h^6)\right)u_i \ . \end{aligned} \tag{34}$$

The error of the velocity ϵ_v can be estimated

$$\epsilon_v=\left[\omega^2h^2\left(\alpha-\frac{1}{2}\right)+\omega^4h^4\left(\frac{1}{24}-\frac{\alpha^3}{2}\right)+\mathcal{O}(h^6)\right]v_i+\left[\omega^4h^3\left(\frac{1}{6}-\frac{\alpha^2}{2}\right)+\mathcal{O}(h^5)\right]u_i \tag{35}$$

and the error of the displacements ϵ_u

$$\epsilon_u=\left[\omega^2h^3\left(\alpha^2-\frac{1}{6}\right)+\mathcal{O}(h^5)\right]v_i+\left[\omega^2h^2\left(\frac{1}{2}-\alpha\right)+\omega^4h^4\left(\frac{1}{24}-\frac{\alpha^3}{2}\right)+\mathcal{O}(h^6)\right]u_i. \tag{36}$$

For $\alpha=1/2$ the second-order terms vanish. The error in this case is described by $1/12\ h^3+\mathcal{O}(h^4)$. In this case, however, the procedure is conditionally stable and a sufficiently low time step must be applied. In the case of large gradients or discontinuities of solutions, a refined mesh is usually used. In such a case a conditional stability can be a serious limitation.

In the case of an unconditionally stable solution scheme we use $\alpha\geq\sqrt{2}/2$. The error is proportional to $(\sqrt{2}-1)/2\,h^2$. In practice we can consider this value as the error of the method with Dirac delta virtual time function.

4 String element carrying a mass

The last term $\delta(x-vt)\,m\,\partial^2u(vt,t)/\partial t^2$ in the motion equation (4) describes the inertial moving mass. $\partial^2u(vt,t)/\partial t^2$ is the vertical acceleration of the moving mass and, at the same time, the acceleration of the point of the string in which the mass is temporarily placed (it is $x=x_0+vt$). The acceleration of the mass $\partial^2u(vt,t)/\partial t^2$ moving with a constant velocity v, according to the Renaudot formula (which in fact is the chain rule of differentiation), results in three terms:

$$\frac{\partial^2u(vt,t)}{\partial t^2} = \left.\frac{\partial^2u(x,t)}{\partial t^2}\right|_{x=vt}+2v\left.\frac{\partial^2u(x,t)}{\partial x\partial t}\right|_{x=vt}+v^2\left.\frac{\partial^2u(x,t)}{\partial x^2}\right|_{x=vt}. \tag{37}$$

Thus we can separate the transverse acceleration, Coriolis acceleration, and centrifugal acceleration, respectively. This is the so-called Renaudot notation for the constant speed v. Another one, the so-called Jakushev notation or approach, finally gives the same result in our case of the constant

mass m.

In our space-time finite element method we formulate equations in terms of velocities. The mass acceleration $\frac{\partial^2 u(vt,t)}{\partial t^2}$ is expressed in terms of velocities as well:

$$\frac{\partial^2 u(vt,t)}{\partial t^2} = \left.\frac{\partial v(x,t)}{\partial t}\right|_{x=vt} + v \left.\frac{\partial v(x,t)}{\partial x}\right|_{x=vt} + v\frac{\mathrm{d}}{\mathrm{d}t}\left[\left.\frac{\partial u(x,t)}{\partial x}\right|_{x=vt} + \frac{\mathrm{d}u_0}{\mathrm{d}x}\right]. \tag{38}$$

After multiplication by m, the first term on the right-hand side of the equation states the real inertia and the second term expresses the forces similar to damping forces.

In the final stage, three resulting matrices are responsible for: transverse inertia, damping forces, and stiffness or potential forces, respectively. The first matrix has a form of the inertia matrix, the second one, after multiplication by a velocity vector, has a form similar to Coriolis forces, and the third one, when multiplied by $\mathbf{v}$, has a form similar to centrifugal forces. We do not call these forces directly, since in the case of straight motion of the mass particle along the bar in axial vibrations we cannot have exactly centrifugal forces, for example. The mathematics are, however, identical. We mention here only that the third matrix appears as a result of initial displacements in time interval.

Let us now follow this idea and treat numerically the right-hand side inertial term of (4). The same mathematical steps as in the case of pure string enable us to integrate the inertial term

$$\int_0^h \int_0^b \mathbf{N}^* m\delta(x - x_0 - vt) \frac{\partial^2 u(x_0 + vt, t)}{\partial t^2} \,\mathrm{d}x\mathrm{d}t \ . \tag{39}$$

Below we use the hat-shaped virtual functions in time. Respective matrices derived with Dirac delta virtual functions are described in [1]. We consider first the integral term of (10). We use the same linear interpolation of the velocity (8). The virtual velocity v^*:

$$v^*(x) = \mathbf{N}^* \mathbf{v}_p = \begin{bmatrix} 1 - \frac{x}{b} \\ \\ \frac{x}{b} \end{bmatrix} \mathbf{v}_p \ . \tag{40}$$

Consequent integration and rearrangement of terms result in characteristic matrices. The moving mass inertia matrix $\mathbf{M}_m$ is given as

$$\mathbf{M}_m = \frac{m}{h} \left[\begin{array}{cc|cc} -(1-\kappa)^2 & -\kappa(1-\kappa) & (1-\kappa)^2 & \kappa(1-\kappa) \\ \\ -\kappa(1-\kappa) & -\kappa^2 & \kappa(1-\kappa) & \kappa^2 \end{array}\right], \tag{41}$$

where $\kappa = (x_0 + vh/2)/b$. x_0 is a starting position of the mass in the space-time element (at $t = t_0$) (see Figure 4). The moving mass damping matrix $\mathbf{C}_m$

$$\mathbf{C}_m = \frac{mv}{b} \left[\begin{array}{cc|cc} -\frac{1}{2}(1-\kappa) & \frac{1}{2}(1-\kappa) & -\frac{1}{2}(1-\kappa) & \frac{1}{2}(1-\kappa) \\ \\ -\frac{1}{2}\kappa & \frac{1}{2}\kappa & -\frac{1}{2}\kappa & \frac{1}{2}\kappa \end{array}\right]. \tag{42}$$

Let us now consider the contribution of $u(x,t)$ and $u(x,0)$ in (10). We integrate by parts

$$\begin{aligned} v\int_0^h\int_0^b \delta(x-x_0-vt)\,\frac{\mathrm{d}}{\mathrm{d}t}\left[\left.\frac{\partial u(x,t)}{\partial x}\right|_{x=vt}+\frac{\mathrm{d}u_0}{\mathrm{d}x}\right]v^*(x)\,\mathrm{d}x\mathrm{d}t \;= \\ =\; -v^2\int_0^h\int_0^b \delta'(x-x_0-vt)\,\left[\left.\frac{\partial u(x,t)}{\partial x}\right|_{x=vt}+\frac{\mathrm{d}u_0}{\mathrm{d}x}\right]v^*(x)\,\mathrm{d}x\mathrm{d}t\;. \end{aligned} \tag{43}$$

Finally we have the stiffness matrix $\mathbf{K}_m$ of the moving mass particle m

$$\mathbf{K}_m=\frac{mhv^2}{6b^2}\left[\begin{array}{cc|cc} 1 & -1 & 2 & -2 \\ & & & \\ -1 & 1 & -2 & 2 \end{array}\right]\;. \tag{44}$$

Since

$$u_0=\left(1-\frac{x}{b}\right)u_3+\frac{x}{b}u_4 \tag{45}$$

and

$$\frac{\mathrm{d}u_0}{\mathrm{d}x}=-\frac{1}{b}u_3+\frac{1}{b}u_4\;, \tag{46}$$

we can write the nodal force vector $\mathbf{e}_m$ of the moving mass

$$\mathbf{e}_m=\frac{mv^2}{b^2}\left[\begin{array}{c} u_L-u_P \\ \\ -u_L+u_P \end{array}\right]\;. \tag{47}$$

u_L and u_R are the displacements in the left and right node in the spatial element. The vector $\mathbf{e}_m$ can also be written with components $\mp mv^2/b\varepsilon_0$.

5 Bernoulli-Euler beam element carrying a mass

The discrete beam element, in both the classical finite element method and space-time finite element method, is more complicated than the string element. Derivation of matrices with the use of Dirac delta virtual time functions are notionally difficult. The product of the Dirac-type virtual function and the Dirac distribution of the mass in space, with the argument varying in time, cause mathematical problems. In this section we use hat-shaped virtual functions in our analysis. They are simple to analyse and are characteristic of lower error rate. The value of this function is constant in time and respective derivatives and double integral can be computed relatively simply.

Mathematical steps will be performed here in the same way as in the string element carrying mass. The beam element results in larger matrices with significantly complicated expressions. In the following we will consider mathematically the first element of the inertia matrix only. All remaining elements of $\mathbf{M}_m$ can be computed matricially. Other matrices, ie. $\mathbf{C}_m$, $\mathbf{M}_m$, and $\mathbf{E}_m$ in (18), are obtained in the same way. Matrices of the element carrying the mass differ in each time step since

the position of the mass particle varies in time. Thus the global matrices must be established in each time step.

We remember that virtual time function v^* in the hat shape is constant in time and in the case of the Bernoulli-Euler beam it has the following form:

$$v_m^*(x,t) = \left(1 - 3\frac{x^2}{b^2} + 2\frac{x^3}{b^3}\right) v_3 + \ldots \ \dot{\varphi}_3 + \ldots \ v_4 + \ldots \ \dot{\varphi}_4 \ . \tag{48}$$

We recognise here the well-known shape functions that describe displacements (or velocities) in terms of nodal displacement and nodal rotations. The same interpolation formulas are applied as real spatial shape functions. Then the elements of the matrix $\mathbf{M}_m$ can be computed. We present here the analysis in the case of the first element $(\cdot)_{11}$ of the inertia matrix only.

$$\begin{aligned}(\mathbf{M}_m)_{11} \ &= \ -\frac{m}{h}\int_0^h \int_0^b \delta(x - x_0 - vt)\left(1 - 3\frac{x^2}{b^2} + 2\frac{x^3}{b^3}\right)^2 \mathrm{d}x\mathrm{d}t \ = \\ &= \ -\frac{m}{h}\int_0^h \int_0^b \left[1 - 3\frac{(x_0+vt)^2}{b^2} + 2\frac{(x_0+vt)^3}{b^3}\right]^2 \mathrm{d}x\mathrm{d}t \ .\end{aligned} \tag{49}$$

We introduce the substitution:

$$s = \frac{x_0 + vt}{b} \quad \text{and} \ \mathrm{d}s = \frac{v}{b}\mathrm{d}t \ . \tag{50}$$

The coefficient $(\mathbf{M}_m)_{11}$ can be written then as

$$(\mathbf{M}_m)_{11} \ = \ -\frac{m}{h}\int_0^h \left(1 - 3s^2 + 2s^3\right)^2 \mathrm{d}s \ = \ -\frac{m}{h}\frac{b}{v}\left(\frac{4}{7}s^7 - 2s^6 + \frac{9}{5}s^5 + s^4 - 2s^3 + s\right)\Big|_0^h \ . \tag{51}$$

Now we return to the variable t:

$$\begin{aligned}(\mathbf{M}_m)_{11} \ = \ -\frac{mb}{hv}\Bigg[\frac{4}{7}\left(\frac{x_0+vt}{b}\right)^7 - \ 2\left(\frac{x_0+vt}{b}\right)^6 + \frac{9}{5}\left(\frac{x_0+vt}{b}\right)^5 + \left(\frac{x_0+vt}{b}\right)^4 - \\ - \ 2\left(\frac{x_0+vt}{b}\right)^3 + \frac{x_0+vt}{b}\Bigg]\Bigg|_0^h \ .\end{aligned} \tag{52}$$

Taking into account the integration limits we have the following form:

$$\begin{aligned}(\mathbf{M}_m)_{11} \ = \ -\frac{m}{560b^6}\Big[560b^6\left(4\kappa^6 - 12\kappa^5 + 9\kappa^4 + 4\kappa^3 - 6\kappa^2 + 1\right) \ + \ 280b^4v^2h^2\left(10\kappa^4 - \right. \\ \left. - \ 20\ \kappa^3 + 9\kappa^2 + 2\kappa - 1\right) \ + \ 21b^2v^4h^4\left(20\kappa^2 - 20\kappa + 3\right) \ + \ 5v^6h^h\Big] \ ,\end{aligned} \tag{53}$$

where

$$\kappa \ = \ \frac{x_0 + vh/2}{b} \quad . \tag{54}$$

Complete matrices carrying mass particles $\mathbf{M}_m$, $\mathbf{C}_m$, $\mathbf{K}_m$, and $\mathbf{E}_m$ in the solution (18), (19) are large. They are listed in the Appendix. We must remember that the first three matrices join velocity vectors in two successive whiles and are composed of two square submatrices, left and right. They have dimensions $n \times 2n$, where n is the total number of degrees of freedom of the structure. Matrix $\mathbf{E}_m$ has a dimension $n \times n$. All matrices given in the Appendix are established for the $m = 1$, so they must be multiplied by real value m. We have also introduced $\xi = vh/b$ and κ given by (54).

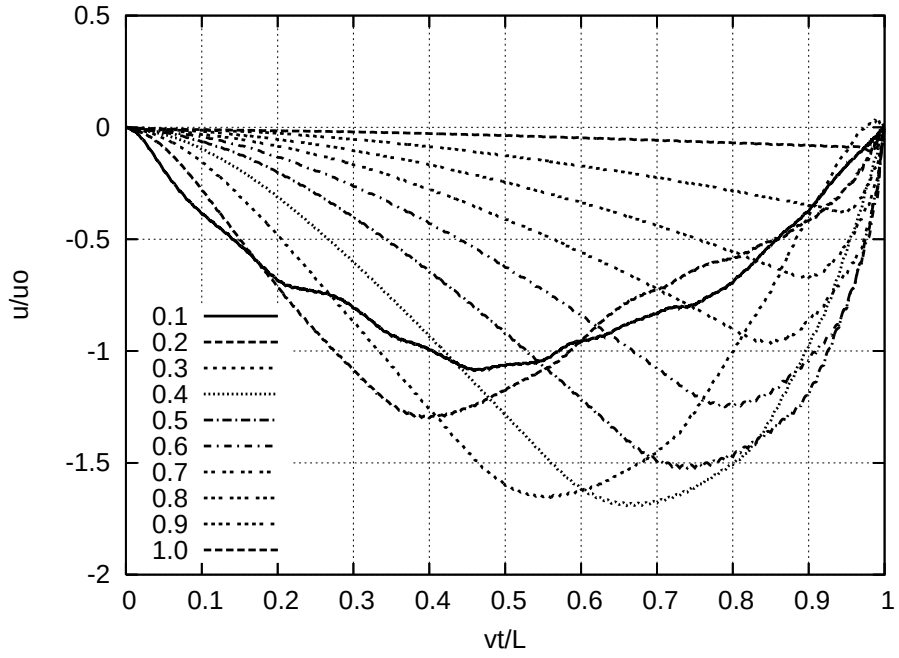

Figure 6: Finite element solution – displacements of the string under the oscillator, with the velocity $v = 0.1 - 1.0c$.

6 Numerical results

Numerical results obtained with the proposed space-time approach can be compared with the semi-analytical solution. We add for information only the plot of oscillator displacements moving over the string (Figure 6). The oscillator spring stiffness was assumed to be high enough to simulate a rigid contact of the mass with the string. Its value was $10^8 - 10^{10}$ times higher than the string vertical stiffness. For higher values, the numerical divergence appeared in the iterative solution. Especially in higher speed ranges the differences of results in comparison with semi-analytical results are noticeable. That is the reason why such an approach cannot be used in analysis or considered in practice.

In our tests performed with the space-time element method the string was discretised by a set of 200 finite elements. The time step h was equal to $b/40v$. It means that the mass passes from joint to joint in 40 time steps. The following data were assumed: the length of the string l=1, the cross-section area A=1, the tension N=1, the mass density ρ=1, the moving mass m=1, and the point force P=1. The following boundary conditions were assumed: $u(0,t) = u(l,t) = 0$. Results obtained by the space-time finite element method are presented in Figure 7. First of all, the numerical solutions exist and they converge to the exact solution. The convergence with the increasing number of finite elements and decreasing time step is slower for higher mass speed range.

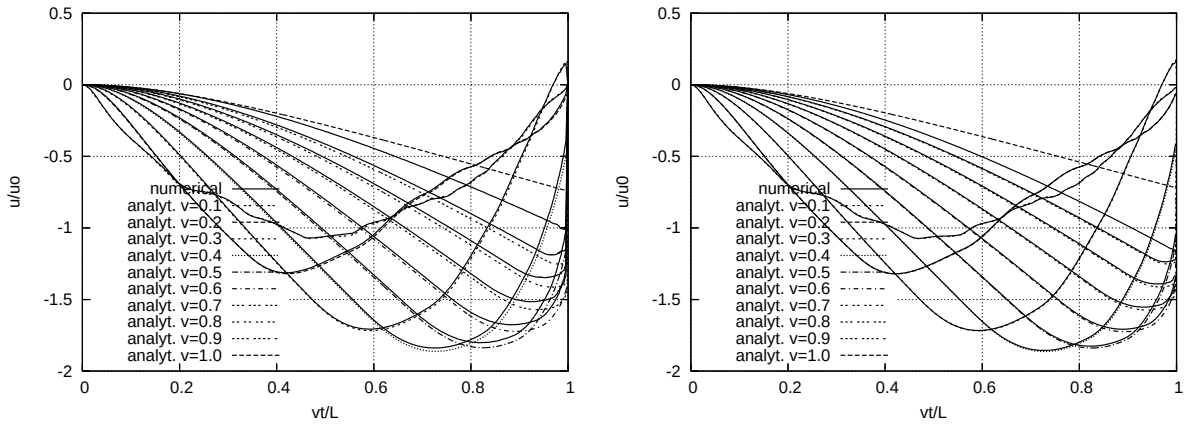

Figure 7: Displacements under the moving mass – space-time finite element solution for a virtual Dirac function with $\alpha = 0.5$ (left) and a virtual hat function (right), compared with the semi-analytical solution.

We can see significantly better accuracy of solutions with the hat virtual functions.

Numerical results of displacements in time of the Bernoulli-Euler simply-supported beam are presented in Figure 8. The following data were applied: E=1.0, A=1.0, I=0.01, l=1.0, ρ=1.0, m=1.0, and P=1.0. The following boundary conditions were assumed in this example: $u(0,t) = u(l,t) = 0$. Additionally, natural boundary conditions were supplied by element interpolation functions: $u''(0,t) = u''(l,t) = 0$. Vertical displacements are related to the static deflection of the middle of the span under the force placed in $x = l/2$. We note the perfect coincidence of the numerical analysis with the hat-shape virtual functions and semi-analytical curves. The Dirac-shape virtual functions result in a small error. Significant decrease of the time step reduces the difference, however, and all three curves coincide.

In the next example, the cantilever beam was subjected to the travelling inertial load. The data were taken from the previous example. The boundary conditions were assumed as follows: $u(0,t) = u'(0,t) = 0$. Additionally, natural boundary conditions were supplied by element interpolation functions: $u''(l,t) = u'''(l,t) = 0$. Figure 9a shows the deflection of the point following the mass and Figure 9b – the deflection of the free end of the beam. Displacements are related to the static deflection of the free end of the beam under the force placed in $x = l$.

We emphasise here that numerical results perfectly coincide with the semi-analytical solution in a wide range of the mass velocity. We applied non-dimensional speed v= up to 0.5, which corresponds with 0.3 of the critical speed. The critical speed means the speed of the force travelling in a cyclic way through a beam, when the vertical deflection increases to infinity. In the case of a moving mass, the critical speed has considerably lower value, and in our example we come close

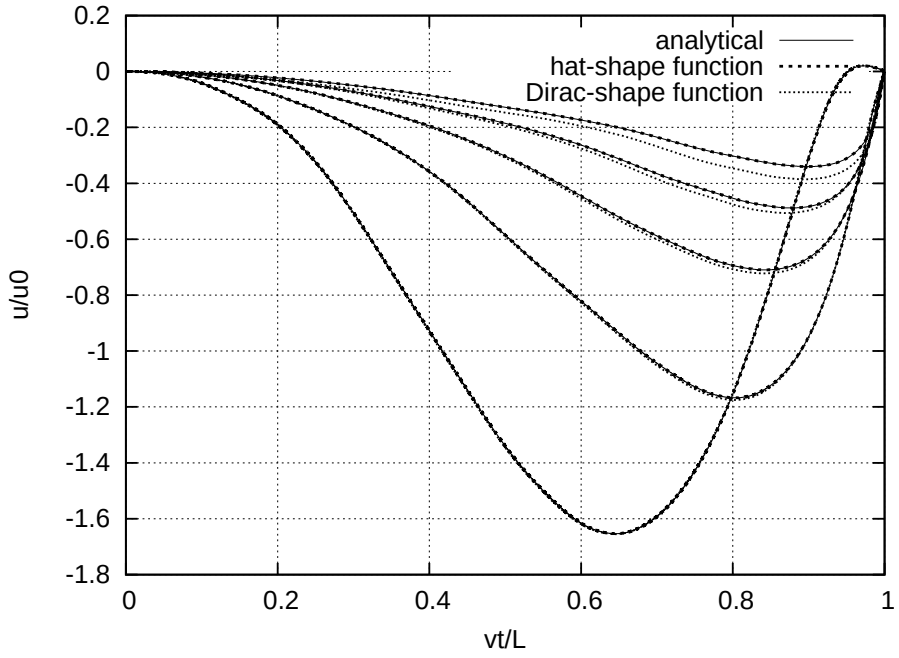

Figure 8: Displacements under the mass moving on the Bernoulli-Euler simply-supported beam at the speed v=0.1, 0.2, ..., 0.5 (numerical and semi-analytical results).

to it.

7 Conclusions

In the paper we propose the space-time element approach to problems with a moving mass. The classical finite element approach does not allow us to obtain satisfactory results. They fail in the case of a string and exhibit very large errors in the case of beams. Typically applied methods of time integration, for example, the Newmark method, fail since the moving inertia term cannot be considered in a continuous way in the time interval. Complex analysis could be performed with the space-time approach. Various virtual functions in time can be applied. They result in a solution scheme characteristic of different accuracy. It is well demonstrated in the case of the mass trajectory plots. At the final stage of the motion the trajectories exhibit jumps (see [8]). In Figure 10 we show the convergence of the semi-analytical solution with increasing number of terms in a series. The jump of the trajectory should also be sufficiently accurate in numerical representations. Jumps in every case of numerical analysis are poorly represented by numerical solutions. In our problem, in the higher speed range jumps are visible in solutions with sufficiently small error. A shorter time step increases the accuracy.

Figure 7 demonstrates that the hat virtual function results in a better convergence. The choice

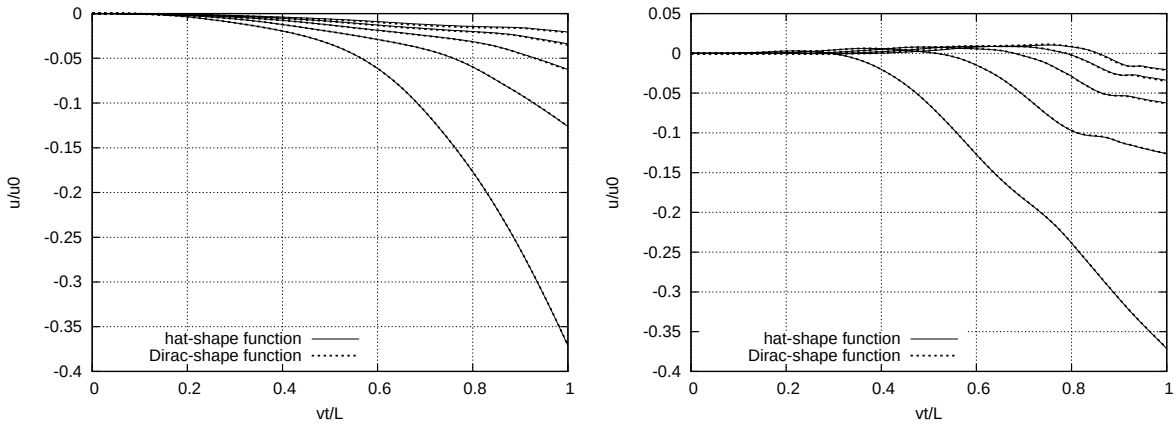

Figure 9: Displacements under the mass moving on the Bernoulli-Euler cantilever beam (a) and displacements of the free end (b) at the speed v=0.1, 0.2, ..., 0.5, with hat-shape and Dirac-shape virtual functions.

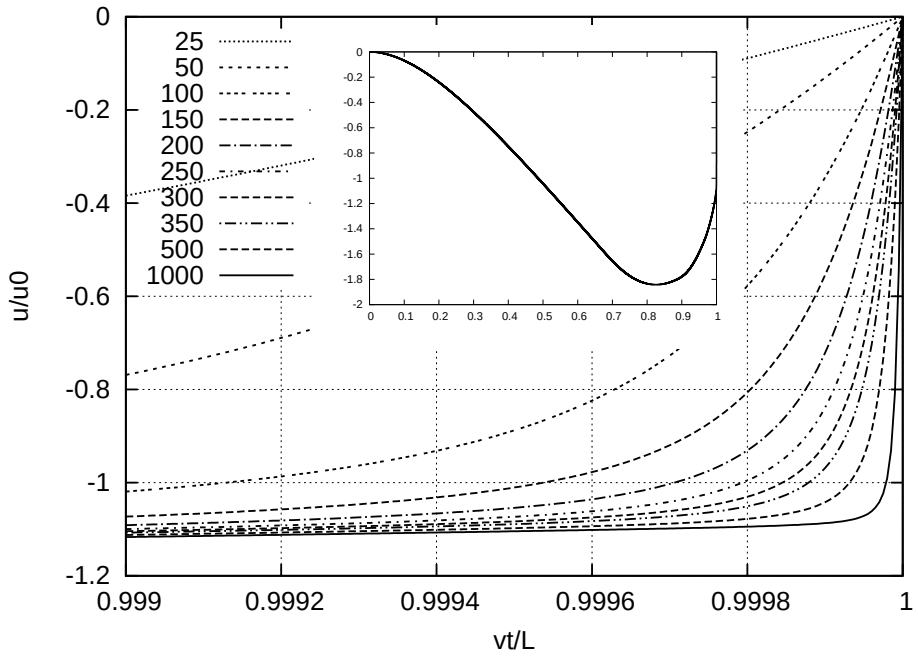

Figure 10: Convergence of displacements under the mass moving on a string with a speed v=0.5c in the semi-analytical solution with increasing number of terms in a series.

of the virtual time step in the form of a hat, instead of the Dirac delta type of this function, significantly improves the quality of the solution. Both cases, i.e. the Dirac delta virtual function with α=1/2 and the hat-shaped virtual function, exhibit theoretically the same estimated error of the method. The two sets of results differ, however. We can say that the error is contributed by and accumulated with different speed because of other stages of the solution scheme: velocity computation or displacement restitution.

Solutions given in the paper are efficient in discrete vibration analysis with travelling mass. Although the problem deals with the mass moving with the constant speed, the same mathematical procedure can be used to derive characteristic matrices in the case of the mass moving with a varying speed. In this case, only additional terms describing the influence of the motion acceleration along the structure must be taken into account. In the present paper these terms are equal to zero.

The perfect coincidence with the semi-analytical solutions proves the efficiency of the space-time approach. The solution method can easily be implemented in the classical finite element code.

References

[1] C.I. Bajer and B. Dyniewicz. Space-time approach to numerical analysis of a string with a moving mass. *Int. J. Numer. Meth. Engng.*, 76(10):1528–1543, 2008.

[2] F.V. Filho. Finite element analysis of structures under moving loads. *The Shock and Vibration Digest*, 10(8):27–35, 1978.

[3] E.C. Ting, J. Genin, and J.H. Ginsberg. A general algorithm for moving mass problems. *J. Sound Vib.*, 33(1):49–58, 1974.

[4] R.S. Ayre, L.S. Jacobsen, and C.S. Hsu. Transverse vibration of one- and two-span beams under the action of a moving mass load. In ASME, editor, *Proc. of the First US Nat. Congr. of Appl. Mech.*, pages 81–90, 1951.

[5] R.F. Keltie and C.C. Cheng. Vibration reduction of the mass-loaded beam. *J. Sound Vibr.*, 187(2):213–228, 1995.

[6] E. Esmailzadeh and M. Ghorashi. Vibration analysis of beams traversed by uniform partially distributed moving mass. *J. Sound Vibr.*, 184(1):9–17, 1995.

[7] B. Dyniewicz and C.I. Bajer. Inertial load moving on a string – discontinuous solution. In W. Szcześniak, editor, *Theoretical Foundations in Civil Engineering*, pages 141–150. OWPW Warsaw, 2007.

[8] B. Dyniewicz and C.I. Bajer. Paradox of the particle's trajectory moving on a string. *Arch. Appl. Mech.*, 2008. DOI: 10.1007/s00419-008-0222-9.

[9] C.I. Bajer. Triangular and tetrahedral space–time finite elements in vibration analysis. *Int. J. Numer. Meth. Engng.*, 23:2031–2048, 1986.

[10] C.I. Bajer. Notes on the stability of non–rectangular space–time finite elements. *Int. J. Numer. Meth. Engng.*, 24:1721–1739, 1987.

[11] C.I. Bajer. Adaptive mesh in dynamic problem by the space–time approach. *Comput. and Struct.*, 33(2):319–325, 1989.

[12] C.I. Bajer, R. Bogacz, and C. Bonthoux. Adaptive space–time elements in the dynamic elastic–viscoplastic problem. *Comput. and Struct.*, 39:415–423, 1991.

[13] C. Bajer. Space–time finite element formulation for the dynamical evolutionary process. *Appl. Math. and Comp. Sci.*, 3(2):251–268, 1993.

[14] C.I. Bajer and C. Bohatier. The soft way method and the velocity formulation. *Comput. and Struct.*, 55(6):1015–1025, 1995.

Matrix $\mathbf{M}_m$ – Bernoulli-Euler beam (left hand square)

$$
\begin{bmatrix}
\begin{array}{l}
-4\kappa^6+12\kappa^5- \\
\kappa^4(5\xi^2+9)+ \\
2\kappa^3(5\xi^2-2)- \\
3\kappa^2(\xi^4+6\xi^2-8)/4+ \\
\kappa\xi^2(3\xi^2-4)/4- \\
(5\xi^6+63\xi^4-280\xi^2+560)/560
\end{array} &
\begin{array}{l}
-2hv\kappa^6/\xi+7hv\kappa^5/\xi- \\
hv\kappa^4(5\xi^2+16)/(2\xi)+ \\
hv\kappa^3(35\xi^2+12)/(6\xi)- \\
hv\kappa^2(3\xi^4+32\xi^2-16)/(8\xi)+ \\
hv\kappa(7\xi^4+8\xi^2-16)/(16\xi)- \\
hv\xi(15\xi^4+336\xi^2-560)/3360
\end{array} &
\begin{array}{l}
4\kappa^6-12\kappa^5+ \\
\kappa^4(5\xi^2+9)+ \\
2\kappa^3(1-5\xi^2)+ \\
3\kappa^2(\xi^4+6\xi^2-4)/4+ \\
\kappa\xi^2(2-3\xi^2)/4+ \\
\xi^2(5\xi^4+63\xi^2-140)/560
\end{array} &
\begin{array}{l}
-2hv\kappa^6/\xi+5hv\kappa^5/\xi- \\
hv\kappa^4(5\xi^2+6)/(2\xi)+ \\
hv\kappa^3(25\xi^2-6)/(6\xi)- \\
hv\kappa^2(3\xi^4+12\xi^2-8)/(8\xi)+ \\
hv\kappa\xi(5\xi^2-4)/16- \\
hv\xi(15\xi^4+126\xi^2-280)/3360
\end{array} \\
\\
\begin{array}{l}
-2hv\kappa^6/\xi+7hv\kappa^5/\xi- \\
hv\kappa^4(5\xi^2+16)/(2\xi)+ \\
hv\kappa^3(35\xi^2+12)/(6\xi)- \\
hv\kappa^2(3\xi^4+32\xi^2-16)/(8\xi)+ \\
hv\kappa(7\xi^4+8\xi^2-16)/(16\xi)- \\
hv\xi(15\xi^4+336\xi^2-560)/3360
\end{array} &
\begin{array}{l}
-h^2v^2\kappa^6/\xi^2+4h^2v^2\kappa^5/\xi^2- \\
h^2v^2\kappa^4(5\xi^2+24)/(4\xi^2)+ \\
2h^2v^2\kappa^3(5\xi^2+6)/(3\xi^2)- \\
h^2v^2\kappa^2(3\xi^4+48\xi^2+16)/(16\xi^2)+ \\
h^2v^2\kappa(\xi^2+4)/4- \\
h^2v^2(15\xi^4+504\xi^2+560)/6720
\end{array} &
\begin{array}{l}
2hv\kappa^6/\xi-7hv\kappa^5/\xi+ \\
hv\kappa^4(5\xi^2+16)/(2\xi)- \\
hv\kappa^3(35\xi^2+18)/(6\xi)+ \\
hv\kappa^2\xi(3\xi^2+32)/8- \\
hv\kappa\xi(7\xi^2+12)/16+ \\
hv\xi^3(5\xi^2+112)/1120
\end{array} &
\begin{array}{l}
-h^2v^2\kappa^6/\xi^2+3h^2v^2\kappa^5/\xi^2- \\
h^2v^2\kappa^4(5\xi^2+12)/(4\xi^2)+ \\
h^2v^2\kappa^3(5\xi^2+2)/(2\xi^2)- \\
3h^2v^2\kappa^2(\xi^2+8)/16+ \\
h^2v^2\kappa(3\xi^2+4)/16- \\
h^2v^2\xi^2(5\xi^2+84)/2240
\end{array} \\
\\
\begin{array}{l}
4\kappa^6-12\kappa^5+ \\
\kappa^4(5\xi^2+9)+ \\
2\kappa^3(1-5\xi^2)+ \\
3\kappa^2(\xi^4+6\xi^2-4)/4+ \\
\kappa\xi^2(2-3\xi^2)/4+ \\
\xi^2(5\xi^4+63\xi^2-140)/560
\end{array} &
\begin{array}{l}
2hv\kappa^6/\xi-7hv\kappa^5/\xi+ \\
hv\kappa^4(5\xi^2+16)/(2\xi)- \\
hv\kappa^3(35\xi^2+18)/(6\xi)+ \\
hv\kappa^2\xi(3\xi^2+32)/8- \\
hv\kappa\xi(7\xi^2+12)/16+ \\
hv\xi^3(5\xi^2+112)/1120
\end{array} &
\begin{array}{l}
-4\kappa^6+12\kappa^5- \\
\kappa^4(5\xi^2+9)+ \\
10\kappa^3\xi^2- \\
3\kappa^2\xi^2(\xi^2+6)/4+ \\
3\kappa\xi^4/4- \\
\xi^4(5\xi^2+63)/560
\end{array} &
\begin{array}{l}
2hv\kappa^6/\xi-5hv\kappa^5/\xi+ \\
hv\kappa^4(5\xi^2+6)/(2\xi)- \\
25hv\kappa^3\xi/6+ \\
3hv\kappa^2\xi(\xi^2+4)/8- \\
5hv\kappa\xi^3/16+ \\
hv\xi^3(5\xi^2+42)/1120
\end{array} \\
\\
\begin{array}{l}
-2hv\kappa^6/\xi+5hv\kappa^5/\xi- \\
hv\kappa^4(5\xi^2+6)/(2\xi)+ \\
hv\kappa^3(25\xi^2-6)/(6\xi)- \\
hv\kappa^2(3\xi^4+12\xi^2-8)/(8\xi)+ \\
hv\kappa\xi(5\xi^2-4)/16- \\
hv\xi(15\xi^4+126\xi^2-280)/3360
\end{array} &
\begin{array}{l}
-h^2v^2\kappa^6/\xi^2+3h^2v^2\kappa^5/\xi^2- \\
h^2v^2\kappa^4(5\xi^2+12)/(4\xi^2)+ \\
h^2v^2\kappa^3(5\xi^2+2)/(2\xi^2)- \\
3h^2v^2\kappa^2(\xi^2+8)/16+ \\
h^2v^2\kappa(3\xi^2+4)/16- \\
h^2v^2\xi^2(5\xi^2+84)/2240
\end{array} &
\begin{array}{l}
2hv\kappa^6/\xi-5hv\kappa^5/\xi+ \\
hv\kappa^4(5\xi^2+6)/(2\xi)- \\
25hv\kappa^3\xi/6+ \\
3hv\kappa^2\xi(\xi^2+4)/8- \\
5hv\kappa\xi^3/16+ \\
hv\xi^3(5\xi^2+42)/1120
\end{array} &
\begin{array}{l}
-h^2v^2\kappa^6/\xi^2+2h^2v^2\kappa^5/\xi^2- \\
h^2v^2\kappa^4(5\xi^2+4)/(4\xi^2)+ \\
5h^2v^2\kappa^3/3- \\
h^2v^2\kappa^2(3\xi^2+8)/16+ \\
h^2v^2\kappa\xi^2/8- \\
h^2v^2\xi^2(5\xi^2+28)/2240
\end{array}
\end{bmatrix}
$$

Matrix $\mathbf{M}_m$ – Bernoulli-Euler beam (right hand square)

$$
\begin{bmatrix}
\begin{array}{l}
4\kappa^6 - 12\kappa^5 + \\
\kappa^4(5\xi^2 + 9) + \\
2\kappa^3(2 - 5\xi^2) + \\
3\kappa^2(\xi^4 + 6\xi^2 - 8)/4 + \\
\kappa\xi^2(4 - 3\xi^2)/4 + \\
(5\xi^6 + 63\xi^4 - 280\xi^2 + 560)/560
\end{array} &
\begin{array}{l}
2hv\kappa^6/\xi - 7hv\kappa^5/\xi + \\
hv\kappa^4(5\xi^2 + 16)/(2\xi) - \\
hv\kappa^3(35\xi^2 + 12)/(6\xi) + \\
hv\kappa^2(3\xi^4 + 32\xi^2 - 16)/(8\xi) - \\
hv\kappa(7\xi^4 + 8\xi^2 - 16)/(16\xi) + \\
hv\xi(15\xi^4 + 336\xi^2 - 560)/3360
\end{array} &
\begin{array}{l}
-4\kappa^6 + 12\kappa^5 - \\
\kappa^4(5\xi^2 + 9) + \\
2\kappa^3(5\xi^2 - 1) - \\
3\kappa^2(\xi^4 + 6\xi^2 - 4)/4 + \\
\kappa\xi^2(3\xi^2 - 2)/4 - \\
\xi^2(5\xi^4 + 63\xi^2 - 140)/560
\end{array} &
\begin{array}{l}
2hv\kappa^6/\xi - 5hv\kappa^5/\xi + \\
hv\kappa^4(5\xi^2 + 6)/(2\xi) + \\
hv\kappa^3(6 - 25\xi^2)/(6\xi) + \\
hv\kappa^2(3\xi^4 + 12\xi^2 - 8)/(8\xi) + \\
hv\kappa\xi(4 - 5\xi^2)/16 + \\
hv\xi(15\xi^4 + 126\xi^2 - 280)/3360
\end{array} \\

\begin{array}{l}
2hv\kappa^6/\xi - 7hv\kappa^5/\xi + \\
hv\kappa^4(5\xi^2 + 16)/(2\xi) - \\
hv\kappa^3(35\xi^2 + 12)/(6\xi) + \\
hv\kappa^2(3\xi^4 + 32\xi^2 - 16)/(8\xi) - \\
hv\kappa(7\xi^4 + 8\xi^2 - 16)/(16\xi) + \\
hv\xi(15\xi^4 + 336\xi^2 - 560)/3360
\end{array} &
\begin{array}{l}
h^2v^2\kappa^6/\xi^2 - 4h^2v^2\kappa^5/\xi^2 + \\
h^2v^2\kappa^4(5\xi^2 + 24)/(4\xi^2) - \\
2h^2v^2\kappa^3(5\xi^2 + 6)/(3\xi^2) + \\
h^2v^2\kappa^2(3\xi^4 + 48\xi^2 + 16)/(16\xi^2) - \\
h^2v^2\kappa(\xi^2 + 4)/4 + \\
h^2v^2(15\xi^4 + 504\xi^2 + 560)/6720
\end{array} &
\begin{array}{l}
-2hv\kappa^6/\xi + 7hv\kappa^5/\xi - \\
hv\kappa^4(5\xi^2 + 16)/(2\xi) + \\
hv\kappa^3(35\xi^2 + 18)/(6\xi) - \\
hv\kappa^2\xi(3\xi^2 + 32)/8 + \\
hv\kappa\xi(7\xi^2 + 12)/16 - \\
hv\xi^3(5\xi^2 + 112)/1120
\end{array} &
\begin{array}{l}
h^2v^2\kappa^6/\xi^2 - 3h^2v^2\kappa^5/\xi^2 + \\
h^2v^2\kappa^4(5\xi^2 + 12)/(4\xi^2) - \\
h^2v^2\kappa^3(5\xi^2 + 2)/(2\xi^2) + \\
3h^2v^2\kappa^2(\xi^2 + 8)/16 - \\
h^2v^2\kappa(3\xi^2 + 4)/16 + \\
h^2v^2\xi^2(5\xi^2 + 84)/2240
\end{array} \\

\begin{array}{l}
-4\kappa^6 + 12\kappa^5 - \\
\kappa^4(5\xi^2 + 9) + \\
2\kappa^3(5\xi^2 - 1) - \\
3\kappa^2(\xi^4 + 6\xi^2 - 4)/4 + \\
\kappa\xi^2(3\xi^2 - 2)/4 - \\
\xi^2(5\xi^4 + 63\xi^2 - 140)/560
\end{array} &
\begin{array}{l}
-2hv\kappa^6/\xi + 7hv\kappa^5/\xi - \\
hv\kappa^4(5\xi^2 + 16)/(2\xi) + \\
hv\kappa^3(35\xi^2 + 18)/(6\xi) - \\
hv\kappa^2\xi(3\xi^2 + 32)/8 + \\
hv\kappa\xi(7\xi^2 + 12)/16 - \\
hv\xi^3(5\xi^2 + 112)/1120
\end{array} &
\begin{array}{l}
4\kappa^6 - 12\kappa^5 + \\
\kappa^4(5\xi^2 + 9) - \\
10\kappa^3\xi^2 + \\
3\kappa^2\xi^2(\xi^2 + 6)/4 - \\
3\kappa\xi^4/4 + \\
\xi^4(5\xi^2 + 63)/560
\end{array} &
\begin{array}{l}
-2hv\kappa^6/\xi + 5hv\kappa^5/\xi - \\
hv\kappa^4(5\xi^2 + 6)/(2\xi) + \\
25hv\kappa^3\xi/6 - \\
3hv\kappa^2\xi(\xi^2 + 4)/8 + \\
5hv\kappa\xi^3/16 - \\
hv\xi^3(5\xi^2 + 42)/1120
\end{array} \\

\begin{array}{l}
2hv\kappa^6/\xi - 5hv\kappa^5/\xi + \\
hv\kappa^4(5\xi^2 + 6)/(2\xi) + \\
hv\kappa^3(6 - 25\xi^2)/(6\xi) + \\
hv\kappa^2(3\xi^4 + 12\xi^2 - 8)/(8\xi) + \\
hv\kappa\xi(4 - 5\xi^2)/16 + \\
hv\xi(15\xi^4 + 126\xi^2 - 280)/3360
\end{array} &
\begin{array}{l}
h^2v^2\kappa^6/\xi^2 - 3h^2v^2\kappa^5/\xi^2 + \\
h^2v^2\kappa^4(5\xi^2 + 12)/(4\xi^2) - \\
h^2v^2\kappa^3(5\xi^2 + 2)/(2\xi^2) + \\
3h^2v^2\kappa^2(\xi^2 + 8)/16 - \\
h^2v^2\kappa(3\xi^2 + 4)/16 + \\
h^2v^2\xi^2(5\xi^2 + 84)/2240
\end{array} &
\begin{array}{l}
-2hv\kappa^6/\xi + 5hv\kappa^5/\xi - \\
hv\kappa^4(5\xi^2 + 6)/(2\xi) + \\
25hv\kappa^3\xi/6 - \\
3hv\kappa^2\xi(\xi^2 + 4)/8 + \\
5hv\kappa\xi^3/16 - \\
hv\xi^3(5\xi^2 + 42)/1120
\end{array} &
\begin{array}{l}
h^2v^2\kappa^6/\xi^2 - 2h^2v^2\kappa^5/\xi^2 + \\
h^2v^2\kappa^4(5\xi^2 + 4)/(4\xi^2) - \\
5h^2v^2\kappa^3/3 + \\
h^2v^2\kappa^2(3\xi^2 + 8)/16 - \\
h^2v^2\kappa\xi^2/8 + \\
h^2v^2\xi^2(5\xi^2 + 28)/2240
\end{array}
\end{bmatrix}
$$

Matrix $\mathbf{C}_m$ – Bernoulli-Euler beam (leftt hand square)

$$
\begin{bmatrix}
12\xi\kappa^5 - 10\xi\kappa^4(\xi+3)+ \\
2\xi\kappa^3(5\xi^2+10\xi+9)- \\
3\xi\kappa^2(\xi^3+5\xi^2+3\xi-2)+ \\
\xi\kappa(3\xi^4+12\xi^3+ \\
18\xi^2-8\xi-24)/4- \\
\xi^2(15\xi^4+105\xi^3+126\xi^2- \\
-140\xi-280)/280
\end{bmatrix}
\begin{bmatrix}
6hv\kappa^5 - hv\kappa^4(5\xi+17)+ \\
hv\kappa^3(15\xi^2+34\xi+42)/3- \\
h\xi v\kappa^2(3\xi^2+17\xi+14)/2+ \\
hv\kappa(15\xi^4+68\xi^3+140\xi^2-160)/40- \\
hv(45\xi^5+357\xi^4+588\xi^3- \\
-1120\xi-1680)/1680
\end{bmatrix}
\begin{bmatrix}
-12\xi\kappa^5 + 10\xi\kappa^4(\xi+3)- \\
2\xi\kappa^3(5\xi^2+10\xi+9)+ \\
3\xi\kappa^2(\xi^3+5\xi^2+3\xi-2)- \\
\xi\kappa(3\xi^4+12\xi^3+18\xi^2-8\xi- \\
24)/4+\xi^2(15\xi^4+105\xi^3+ \\
+126\xi^2-140\xi-280)/280
\end{bmatrix}
\begin{bmatrix}
6hv\kappa^5 - hv\kappa^4(5\xi+13)+ \\
hv\kappa^3(15\xi^2+26\xi+18)/3- \\
hv\kappa^2(3\xi^3+13\xi^2+6\xi-6)/2+ \\
hv\kappa(15\xi^4+52\xi^3+60\xi^2-40\xi- \\
-80)/40-h\xi v(45\xi^4+273\xi^3+ \\
+252\xi^2-420\xi-560)/1680
\end{bmatrix}
$$

$$
\begin{bmatrix}
6hv\kappa^5 - hv\kappa^4(5\xi+18)+ \\
hv\kappa^3(5\xi^2+12\xi+18)- \\
3hv\kappa^2(\xi^3+6\xi^2+6\xi+4)/2+ \\
h\xi v\kappa(15\xi^3+72\xi^2+180\xi+ \\
+80)/40-h\xi^2 v(15\xi^3+126\xi^2+ \\
+252\xi+280)/560
\end{bmatrix}
\begin{bmatrix}
3h^2v^2\kappa^5/\xi - 5h^2v^2\kappa^4(\xi+4)/(2\xi)+ \\
h^2v^2\kappa^3(15\xi^2+40\xi+72)/(6\xi)- \\
h^2v^2\kappa^2(3\xi^3+20\xi^2+24\xi+24)/(4\xi)+ \\
h^2v^2\kappa(3\xi^4+16\xi^3+48\xi^2+ \\
+32\xi+16)/(16\xi)- \\
h^2v^2(45\xi^4+420\xi^3+1008\xi^2+ \\
+1680\xi+560)/3360
\end{bmatrix}
\begin{bmatrix}
-6hv\kappa^5 + hv\kappa^4(5\xi+18)- \\
hv\kappa^3(5\xi^2+12\xi+18)+ \\
3hv\kappa^2(\xi^3+6\xi^2+6\xi+4)/2- \\
h\xi v\kappa(15\xi^3+72\xi^2+180\xi+ \\
+80)/40+h\xi^2 v(15\xi^3+126\xi^2+ \\
+252\xi+280)/560
\end{bmatrix}
\begin{bmatrix}
3h^2v^2\kappa^5/\xi - h^2v^2\kappa^4(5\xi+16)/(2\xi)+ \\
h^2v^2\kappa^3(15\xi^2+32\xi+42)/(6\xi)- \\
h^2v^2\kappa^2(3\xi^3+16\xi^2+14\xi+8)/(4\xi)+ \\
h^2v^2\kappa(45\xi^3+192\xi^2+420\xi+ \\
+160)/240-h^2\xi v^2(45\xi^3+336\xi^2+ \\
+588\xi+560)/3360
\end{bmatrix}
$$

$$
\begin{bmatrix}
-12\xi\kappa^5 + 10\xi\kappa^4(\xi+3)- \\
2\xi\kappa^3(5\xi^2+10\xi+9)+ \\
3\xi^2\kappa^2(\xi^2+5\xi+3)- \\
3\xi^3\kappa(\xi^2+4\xi+6)/4+ \\
3\xi^4(5\xi^2+35\xi+42)/280
\end{bmatrix}
\begin{bmatrix}
-6hv\kappa^5 + hv\kappa^4(5\xi+17)- \\
hv\kappa^3(15\xi^2+34\xi+42)/3+ \\
hv\kappa^2(3\xi^3+17\xi^2+14\xi+6)/2- \\
h\xi v\kappa(15\xi^3+68\xi^2+140\xi+40)/40+ \\
h\xi^2 v(15\xi^3+119\xi^2+196\xi+140)/560
\end{bmatrix}
\begin{bmatrix}
12\xi\kappa^5 - 10\xi\kappa^4(\xi+3)+ \\
2\xi\kappa^3(5\xi^2+10\xi+9)- \\
3\xi^2\kappa^2(\xi^2+5\xi+3)+ \\
3\xi^3\kappa(\xi^2+4\xi+6)/4- \\
3\xi^4(5\xi^2+35\xi+42)/280
\end{bmatrix}
\begin{bmatrix}
-6hv\kappa^5 + hv\kappa^4(5\xi+13)- \\
hv\kappa^3(15\xi^2+26\xi+18)/3+ \\
h\xi v\kappa^2(3\xi^2+13\xi+6)/2- \\
h\xi^2 v\kappa(15\xi^2+52\xi+60)/40+ \\
h\xi^3 v(15\xi^2+91\xi+84)/560
\end{bmatrix}
$$

$$
\begin{bmatrix}
6hv\kappa^5 - hv\kappa^4(5\xi+12)+ \\
hv\kappa^3(5\xi^2+8\xi+6)- \\
3h\xi v\kappa^2(\xi^2+4\xi+2)/2+ \\
3h\xi^2 v\kappa(5\xi^2+16\xi+20)/40- \\
3h\xi^3 v(5\xi^2+28\xi+28)/560
\end{bmatrix}
\begin{bmatrix}
3h^2v^2\kappa^5/\xi - h^2v^2\kappa^4(5\xi+14)/(2\xi)+ \\
h^2v^2\kappa^3(15\xi^2+28\xi+30)/(6\xi)- \\
h^2v^2\kappa^2(3\xi^3+14\xi^2+10\xi+4)/(4\xi)+ \\
h^2v^2\kappa(45\xi^3+168\xi^2+300\xi+80)/240- \\
h^2\xi v^2(45\xi^3+294\xi^2+420\xi+280)/3360
\end{bmatrix}
\begin{bmatrix}
-6hv\kappa^5 + hv\kappa^4(5\xi+12)- \\
hv\kappa^3(5\xi^2+8\xi+6)+ \\
3h\xi v\kappa^2(\xi^2+4\xi+2)/2- \\
3h\xi^2 v\kappa(5\xi^2+16\xi+20)/40+ \\
3h\xi^3 v(5\xi^2+28\xi+28)/560
\end{bmatrix}
\begin{bmatrix}
3h^2v^2\kappa^5/\xi - 5h^2v^2\kappa^4(\xi+2)/(2\xi)+ \\
h^2v^2\kappa^3(15\xi^2+20\xi+12)/(6\xi)- \\
h^2v^2\kappa^2(3\xi^2+10\xi+4)/4+ \\
+h^2\xi v^2\kappa(3\xi^2+8\xi+8)/16- \\
h^2\xi^2v^2(15\xi^2+70\xi+56)/1120
\end{bmatrix}
$$

Matrix $\mathbf{C}_m$ – Bernoulli-Euler beam (right hand square)

$$
\begin{bmatrix}
12\xi\kappa^5+10\xi\kappa^4(\xi-3)+ & 6hv\kappa^5+hv\kappa^4(5\xi-17)+ & -12\xi\kappa^5+10\xi\kappa^4(3-\xi)- & 6hv\kappa^5+hv\kappa^4(5\xi-13)+\\
2\xi\kappa^3(5\xi^2-10\xi+9)+ & hv\kappa^3(15\xi^2-34\xi+42)/3+ & 2\xi\kappa^3(5\xi^2-10\xi+9)- & hv\kappa^3(15\xi^2-26\xi+18)/3+\\
3\xi\kappa^2(\xi^3-5\xi^2+3\xi+2)+ & h\xi v\kappa^2(3\xi^2-17\xi+14)/2+ & 3\xi\kappa^2(\xi^3-5\xi^2+3\xi+2)- & hv\kappa^2(3\xi^3-13\xi^2+6\xi+6)/2+\\
\xi\kappa(3\xi^4-12\xi^3+ & hv\kappa(15\xi^4-68\xi^3+140\xi^2-160)/40+ & \xi\kappa(3\xi^4-12\xi^3+18\xi^2+ & hv\kappa(15\xi^4-52\xi^3+60\xi^2+\\
18\xi^2+8\xi-24)/4+ & hv(45\xi^5-357\xi^4+588\xi^3-1120\xi+ & 8\xi-24)/4-\xi^2(15\xi^4-105\xi^3+ & 40\xi-80)/40+h\xi v(45\xi^4-273\xi^3+\\
\xi^2(15\xi^4-105\xi^3+126\xi^2+ & +1680)/1680 & 126\xi^2+140\xi-280)/280 & 252\xi^2+420\xi-560)/1680\\
+140\xi-280)/280 & & & \\
\\
6hv\kappa^5+hv\kappa^4(5\xi-18)+ & 3h^2v^2\kappa^5/\xi+5h^2v^2\kappa^4(\xi-4)/(2\xi)+ & -6hv\kappa^5+hv\kappa^4(18-5\xi)- & 3h^2v^2\kappa^5/\xi+h^2v^2\kappa^4(5\xi-16)/\\
hv\kappa^3(5\xi^2-12\xi+18)+ & h^2v^2\kappa^3(15\xi^2-40\xi+72)/(6\xi)+ & hv\kappa^3(5\xi^2-12\xi+18)- & /(2\xi)+h^2v^2\kappa^3(15\xi^2-32\xi+\\
3hv\kappa^2(\xi^3-6\xi^2+6\xi-4)/2+ & h^2v^2\kappa^2(3\xi^3-20\xi^2+24\xi-24)/(4\xi)+ & 3hv\kappa^2(\xi^3-6\xi^2+6\xi-4)/2- & +42)/(6\xi)+h^2v^2\kappa^2\cdot\\
h\xi v\kappa(15\xi^3-72\xi^2+180\xi- & h^2v^2\kappa(3\xi^4-16\xi^3+48\xi^2-32\xi+ & h\xi v\kappa(15\xi^3-72\xi^2+ & \cdot(3\xi^3-16\xi^2+14\xi-8)/(4\xi)+\\
80)/40+h\xi^2v(15\xi^3-126\xi^2+ & +16)/(16\xi)+h^2v^2(45\xi^4-420\xi^3+ & 180\xi-80)/40-h\xi^2v(15\xi^3- & h^2v^2\kappa(45\xi^3-192\xi^2+420\xi-\\
+252\xi-280)/560 & +1008\xi^2-1680\xi+560)/3360 & -126\xi^2+252\xi-280)/560 & -160)/240+h^2\xi v^2(45\xi^3-\\
 & & & -336\xi^2+588\xi-560)/3360\\
\\
-12\xi\kappa^5+10\xi\kappa^4(3-\xi)- & -6hv\kappa^5+hv\kappa^4(17-5\xi)- & 12\xi\kappa^5+10\xi\kappa^4(\xi-3)+ & -6hv\kappa^5+hv\kappa^4(13-5\xi)-\\
2\xi\kappa^3(5\xi^2-10\xi+9)- & hv\kappa^3(15\xi^2-34\xi+42)/3- & 2\xi\kappa^3(5\xi^2-10\xi+9)+ & hv\kappa^3(15\xi^2-26\xi+18)/3-\\
3\xi^2\kappa^2(\xi^2-5\xi+3)- & hv\kappa^2(3\xi^3-17\xi^2+14\xi-6)/2- & 3\xi^2\kappa^2(\xi^2-5\xi+3)+ & h\xi v\kappa^2(3\xi^2-13\xi+6)/2-\\
3\xi^3\kappa(\xi^2-4\xi+6)/4- & h\xi v\kappa(15\xi^3-68\xi^2+140\xi-40)/40- & 3\xi^3\kappa(\xi^2-4\xi+6)/4+ & h\xi^2v\kappa(15\xi^2-52\xi+60)/40-\\
3\xi^4(5\xi^2-35\xi+42)/280 & h\xi^2v(15\xi^3-119\xi^2+196\xi-140)/560 & 3\xi^4(5\xi^2-35\xi+42)/280 & h\xi^3v(15\xi^2-91\xi+84)/560\\
\\
6hv\kappa^5+hv\kappa^4(5\xi-12)+ & 3h^2v^2\kappa^5/\xi+h^2v^2\kappa^4(5\xi-14)/(2\xi)+ & -6hv\kappa^5+hv\kappa^4(12-5\xi)- & 3h^2v^2\kappa^5/\xi+5h^2v^2\kappa^4(\xi-2)/(2\xi)+\\
hv\kappa^3(5\xi^2-8\xi+6)+ & h^2v^2\kappa^3(15\xi^2-28\xi+30)/(6\xi)+ & hv\kappa^3(5\xi^2-8\xi+6)- & h^2v^2\kappa^3(15\xi^2-20\xi+12)/(6\xi)+\\
3h\xi v\kappa^2(\xi^2-4\xi+2)/2+ & h^2v^2\kappa^2(3\xi^3-14\xi^2+10\xi-4)/(4\xi)+ & 3h\xi v\kappa^2(\xi^2-4\xi+2)/2- & h^2v^2\kappa^2(3\xi^2-10\xi+4)/4+\\
3h\xi^2v\kappa(5\xi^2-16\xi+20)/40+ & h^2v^2\kappa(45\xi^3-168\xi^2+300\xi-80)/240+ & 3h\xi^2v\kappa(5\xi^2-16\xi+20)/40- & h^2\xi v^2\kappa(3\xi^2-8\xi+8)/16+\\
3h\xi^3v(5\xi^2-28\xi+28)/560 & h^2\xi v^2(45\xi^3-294\xi^2+420\xi-280)/3360 & 3h\xi^3v(5\xi^2-28\xi+28)/560 & h^2\xi^2v^2(15\xi^2-70\xi+56)/1120
\end{bmatrix}
$$

Matrix $\mathbf{K}_m$ – Bernoulli-Euler beam (left hand square)

$$8\xi^2\kappa^4 + 4\xi^2\kappa^3(\xi - 4) +$$
$$6\xi^2\kappa^2(3\xi^2 - 5\xi + 5)/5 +$$
$$\xi^2\kappa(6\xi^3 - 36\xi^2 + 15\xi + 40)/10 +$$
$$\xi^2(12\xi^4 - 42\xi^3 + 63\xi^2 +$$
$$+70\xi - 280)/140$$

$$4h\xi v\kappa^4 +$$
$$2h\xi v\kappa^3(3\xi - 13)/3 +$$
$$h\xi v\kappa^2(36\xi^2 - 65\xi + 80)/20 +$$
$$h\xi v\kappa(6\xi^3 - 39\xi^2 + 20\xi + 40)/20 +$$
$$h\xi v(72\xi^4 - 273\xi^3 + 504\xi^2 +$$
$$420\xi - 2240)/1680$$

$$-8\xi^2\kappa^4 +$$
$$4\xi^2\kappa^3(4 - \xi) -$$
$$6\xi^2\kappa^2(3\xi^2 - 5\xi + 5)/5 -$$
$$\xi^2\kappa(6\xi^3 - 36\xi^2 + 15\xi + 40)/10 -$$
$$\xi^2(12\xi^4 - 42\xi^3 + 63\xi^2 +$$
$$+70\xi - 280)/140$$

$$4h\xi v\kappa^4 +$$
$$2h\xi v\kappa^3(3\xi - 11)/3 +$$
$$h\xi v\kappa^2(36\xi^2 - 55\xi + 40)/20 +$$
$$h\xi v\kappa(6\xi^3 - 33\xi^2 + 10\xi + 40)/20 +$$
$$h\xi v(72\xi^4 - 231\xi^3 +$$
$$252\xi^2 + 420\xi - 1120)/1680$$

$$4h\xi v\kappa^4 +$$
$$2h\xi v\kappa^3(\xi - 5) +$$
$$h\xi v\kappa^2(36\xi^2 - 75\xi + 160)/20 +$$
$$h\xi v\kappa(6\xi^3 - 45\xi^2 + 40\xi - 40)/20 +$$
$$h\xi^2 v(24\xi^3 - 105\xi^2 + 336\xi -$$
$$-140)/560$$

$$2h^2v^2\kappa^4 + h^2v^2\kappa^3(3\xi - 16)/3 +$$
$$h^2v^2\kappa^2(27\xi^2 - 60\xi + 140)/30 +$$
$$h^2v^2\kappa(9\xi^3 - 72\xi^2 + 70\xi - 80)/60 +$$
$$h^2\xi v^2(9\xi^3 - 42\xi^2 + 147\xi - 70)/420$$

$$-4h\xi v\kappa^4 +$$
$$2h\xi v\kappa^3(5 - \xi) -$$
$$h\xi v\kappa^2(36\xi^2 - 75\xi + 160)/20 -$$
$$h\xi v\kappa(6\xi^3 - 45\xi^2 + 40\xi - 40)/20 -$$
$$h\xi^2 v(24\xi^3 - 105\xi^2 + 336\xi - 140)/560$$

$$2h^2v^2\kappa^4 +$$
$$h^2v^2\kappa^3(3\xi - 14)/3 +$$
$$h^2v^2\kappa^2(54\xi^2 - 105\xi + 200)/60 +$$
$$h^2v^2\kappa(9\xi^3 - 63\xi^2 + 50\xi - 40)/60 +$$
$$h^2\xi v^2(36\xi^3 - 147\xi^2 + 420\xi -$$
$$-140)/1680$$

$$-8\xi^2\kappa^4 +$$
$$4\xi^2\kappa^3(4 - \xi) -$$
$$6\xi^2\kappa^2(3\xi^2 - 5\xi + 5)/5 -$$
$$3\xi^3\kappa(2\xi^2 - 12\xi + 5)/10 -$$
$$3\xi^4(4\xi^2 - 14\xi + 21)/140$$

$$-4h\xi v\kappa^4 +$$
$$2h\xi v\kappa^3(13 - 3\xi)/3 -$$
$$h\xi v\kappa^2(36\xi^2 - 65\xi + 80)/20 -$$
$$h\xi^2 v\kappa(6\xi^2 - 39\xi + 20)/20 -$$
$$h\xi^3 v(24\xi^2 - 91\xi + 168)/560$$

$$8\xi^2\kappa^4 +$$
$$4\xi^2\kappa^3(\xi - 4) +$$
$$6\xi^2\kappa^2(3\xi^2 - 5\xi + 5)/5 +$$
$$3\xi^3\kappa(2\xi^2 - 12\xi + 5)/10 +$$
$$3\xi^4(4\xi^2 - 14\xi + 21)/140$$

$$-4h\xi v\kappa^4 +$$
$$2h\xi v\kappa^3(11 - 3\xi)/3 -$$
$$h\xi v\kappa^2(36\xi^2 - 55\xi + 40)/20 -$$
$$h\xi^2 v\kappa(6\xi^2 - 33\xi + 10)/20 -$$
$$h\xi^3 v(24\xi^2 - 77\xi + 84)/560$$

$$4h\xi v\kappa^4 +$$
$$2h\xi v\kappa^3(\xi - 3) +$$
$$h\xi v\kappa^2(36\xi^2 - 45\xi + 40)/20 +$$
$$h\xi^2 v\kappa(6\xi^2 - 27\xi + 10)/20 +$$
$$3h\xi^3 v(8\xi^2 - 21\xi + 28)/560$$

$$2h^2v^2\kappa^4 +$$
$$h^2v^2\kappa^3(3\xi - 10)/3 +$$
$$h^2v^2\kappa^2(54\xi^2 - 75\xi + 80)/60 +$$
$$h^2\xi v^2\kappa(9\xi^2 - 45\xi + 20)/60 +$$
$$h^2\xi^2v^2(12\xi^2 - 35\xi + 56)/560$$

$$-4h\xi v\kappa^4 +$$
$$2h\xi v\kappa^3(3 - \xi) -$$
$$h\xi v\kappa^2(36\xi^2 - 45\xi + 40)/20 -$$
$$h\xi^2 v\kappa(6\xi^2 - 27\xi + 10)/20 -$$
$$3h\xi^3 v(8\xi^2 - 21\xi + 28)/560$$

$$2h^2v^2\kappa^4 +$$
$$h^2v^2\kappa^3(3\xi - 8)/3 +$$
$$h^2v^2\kappa^2(27\xi^2 - 30\xi + 20)/30 +$$
$$h^2\xi v^2\kappa(9\xi^2 - 36\xi + 10)/60 +$$
$$h^2\xi^2v^2(3\xi^2 - 7\xi + 7)/140$$

Matrix $\mathbf{K}_m$ – Bernoulli-Euler beam (right hand square)

$$
\begin{bmatrix}
4\xi^2\kappa^4 + 4\xi^2\kappa^3(\xi-2)+ & 2h\xi v\kappa^4 + h\xi v\kappa^3(6\xi-13)/3+ & -4\xi^2\kappa^4 + 4\xi^2\kappa^3(2-\xi)- & 2h\xi v\kappa^4 + h\xi v\kappa^3(6\xi-11)/3+ \\
3\xi^2\kappa^2(4\xi^2-10\xi+5)/5+ & h\xi v\kappa^2(24\xi^2-65\xi+40)/20+ & 3\xi^2\kappa^2(4\xi^2-10\xi+5)/5- & h\xi v\kappa^2(24\xi^2-55\xi+20)/20+ \\
\xi^2\kappa(6\xi^3-24\xi^2+15\xi+20)/10+ & h\xi v\kappa(3\xi^3-13\xi^2+10\xi+10)/10+ & \xi^2\kappa(6\xi^3-24\xi^2+15\xi+20)/10- & h\xi v\kappa(3\xi^3-11\xi^2+5\xi+10)/10+ \\
\xi^2(9\xi^4-42\xi^3+42\xi^2+70\xi- & h\xi v(54\xi^4-273\xi^3+336\xi^2+ & \xi^2(9\xi^4-42\xi^3+ & h\xi v(54\xi^4-231\xi^3+ \\
-140)/140 & +420\xi-1120)/1680 & 42\xi^2+70\xi-140)/140 & 168\xi^2+420\xi-560)/1680 \\
\\
2h\xi v\kappa^4 + h\xi v\kappa^3(2\xi-5)+ & h^2v^2\kappa^4 + h^2v^2\kappa^3(3\xi-8)/3+ & -2h\xi v\kappa^4 + h\xi v\kappa^3(5-2\xi)- & h^2v^2\kappa^4 + h^2v^2\kappa^3(3\xi-7)/3+ \\
h\xi v\kappa^2(24\xi^2-75\xi+80)/20+ & h^2v^2\kappa^2(9\xi^2-30\xi+35)/15+ & h\xi v\kappa^2(24\xi^2-75\xi+80)/20- & h^2v^2\kappa^2(36\xi^2-105\xi+100)/60+ \\
h\xi v\kappa(3\xi^3-15\xi^2+20\xi-10)/10+ & h^2v^2\kappa(9\xi^3-48\xi^2+70\xi-40)/60+ & h\xi v\kappa(3\xi^3-15\xi^2+20\xi-10)/10- & h^2v^2\kappa(9\xi^3-42\xi^2+ \\
h\xi^2v(18\xi^3-105\xi^2+224\xi- & h^2\xi v^2(27\xi^3-168\xi^2+392\xi- & h\xi^2v(18\xi^3-105\xi^2+224\xi- & 50\xi-20)/60+ \\
-140)/560 & -280)/1680 & -140)/560 & h^2\xi v^2(27\xi^3-147\xi^2+280\xi- \\
 & & & -140)/1680 \\
\\
-4\xi^2\kappa^4 + 4\xi^2\kappa^3(2-\xi)- & -2h\xi v\kappa^4 + h\xi v\kappa^3(13-6\xi)/3- & 4\xi^2\kappa^4 + 4\xi^2\kappa^3(\xi-2)+ & -2h\xi v\kappa^4 + h\xi v\kappa^3(11-6\xi)/3- \\
3\xi^2\kappa^2(4\xi^2-10\xi+5)/5- & h\xi v\kappa^2(24\xi^2-65\xi+40)/20- & 3\xi^2\kappa^2(4\xi^2-10\xi+5)/5+ & h\xi v\kappa^2(24\xi^2-55\xi+20)/20- \\
3\xi^3\kappa(2\xi^2-8\xi+5)/10- & h\xi^2v\kappa(3\xi^2-13\xi+10)/10- & 3\xi^3\kappa(2\xi^2-8\xi+5)/10+ & h\xi^2v\kappa(3\xi^2-11\xi+5)/10- \\
3\xi^4(3\xi^2-14\xi+14)/140 & h\xi^3v(18\xi^2-91\xi+112)/560 & 3\xi^4(3\xi^2-14\xi+14)/140 & h\xi^3v(18\xi^2-77\xi+56)/560 \\
\\
2h\xi v\kappa^4 + h\xi v\kappa^3(2\xi-3)+ & h^2v^2\kappa^4 + h^2v^2\kappa^3(3\xi-5)/3+ & -2h\xi v\kappa^4 + h\xi v\kappa^3(3-2\xi)- & h^2v^2\kappa^4 + h^2v^2\kappa^3(3\xi-4)/3+ \\
h\xi v\kappa^2(24\xi^2-45\xi+20)/20+ & h^2v^2\kappa^2(36\xi^2-75\xi+40)/60+ & h\xi v\kappa^2(24\xi^2-45\xi+20)/20- & h^2v^2\kappa^2(9\xi^2-15\xi+5)/15+ \\
h\xi^2v\kappa(3\xi^2-9\xi+5)/10+ & h^2\xi v^2\kappa(9\xi^2-30\xi+20)/60+ & h\xi^2v\kappa(3\xi^2-9\xi+5)/10- & h^2\xi v^2\kappa(9\xi^2-24\xi+10)/60+ \\
h\xi^3v(18\xi^2-63\xi+56)/560 & h^2\xi^2v^2(27\xi^2-105\xi+112)/1680 & h\xi^3v(18\xi^2-63\xi+56)/560 & h^2\xi^2v^2(27\xi^2-84\xi+56)/1680
\end{bmatrix}
$$

Matrix $\mathbf{E}_m$ – Bernoulli-Euler beam

$$
\begin{bmatrix}
24\xi^2\kappa^4/h- & 12\xi v\kappa^4- & -24\xi^2\kappa^4/h+ & 12\xi v\kappa^4- \\
48\xi^2\kappa^3/h+ & 26\xi v\kappa^3+ & 48\xi^2\kappa^3/h- & 22\xi v\kappa^3+ \\
6\xi^2\kappa^2(2\xi^2+3)/h+ & 6\xi v\kappa^2(\xi^2+2)+ & 6\xi^2\kappa^2(2\xi^2+3)/h+ & 6\xi v\kappa^2(\xi^2+1)+ \\
12\xi^2\kappa(1-\xi^2)/h+ & \xi v\kappa(12-13\xi^2)/2+ & 12\xi^2\kappa(\xi^2-1)/h- & \xi v\kappa(12-11\xi^2)/2+ \\
3\xi^2(\xi^4+5\xi^2-20)/(10h) & \xi v(3\xi^4+20\xi^2-80)/20 & 3\xi^2(\xi^4+5\xi^2-20)/(10h) & \xi v(3\xi^4+10\xi^2-40)/20 \\
\\
12\xi v\kappa^4- & 6hv^2\kappa^4- & -12\xi v\kappa^4+ & 6hv^2\kappa^4- \\
30\xi v\kappa^3+ & 16hv^2\kappa^3+ & 30\xi v\kappa^3- & 14hv^2\kappa^3+ \\
6\xi v\kappa^2(\xi^2+4)- & hv^2\kappa^2(3\xi^2+14)- & 6\xi v\kappa^2(\xi^2+4)+ & hv^2\kappa^2(3\xi^2+10)- \\
3\xi v\kappa(5\xi^2+4)/2+ & 4hv^2\kappa(\xi^2+1)+ & 3\xi v\kappa(5\xi^2+4)/2- & hv^2\kappa(7\xi^2+4)/2+ \\
\xi^3 v(3\xi^2+40)/20 & h\xi^2v^2(9\xi^2+140)/120 & \xi^3 v(3\xi^2+40)/20 & h\xi^2v^2(9\xi^2+100)/120 \\
\\
-24\xi^2\kappa^4/h+ & -12\xi v\kappa^4+ & 24\xi^2\kappa^4/h- & -12\xi v\kappa^4+ \\
48\xi^2\kappa^3/h- & 26\xi v\kappa^3- & 48\xi^2\kappa^3/h+ & 22\xi v\kappa^3- \\
6\xi^2\kappa^2(2\xi^2+3)/h+ & 6\xi v\kappa^2(\xi^2+2)+ & 6\xi^2\kappa^2(2\xi^2+3)/h- & 6\xi v\kappa^2(\xi^2+1)+ \\
12\xi^4\kappa/h- & 13\xi^3 v\kappa/2- & 12\xi^4\kappa/h+ & 11\xi^3 v\kappa/2- \\
3\xi^4(\xi^2+5)/(10h) & \xi^3 v(3\xi^2+20)/20 & 3\xi^4(\xi^2+5)/(10h) & \xi^3 v(3\xi^2+10)/20 \\
\\
12\xi v\kappa^4- & 6hv^2\kappa^4- & -12\xi v\kappa^4+ & 6hv^2\kappa^4- \\
18\xi v\kappa^3+ & 10hv^2\kappa^3+ & 18\xi v\kappa^3- & 8hv^2\kappa^3+ \\
6\xi v\kappa^2(\xi^2+1)- & hv^2\kappa^2(3\xi^2+4)- & 6\xi v\kappa^2(\xi^2+1)+ & hv^2\kappa^2(3\xi^2+2)- \\
9\xi^3 v\kappa/2+ & 5h\xi^2v^2\kappa/2+ & 9\xi^3 v\kappa/2- & 2h\xi^2v^2\kappa+ \\
\xi^3 v(3\xi^2+10)/20 & h\xi^2v^2(9\xi^2+40)/120 & \xi^3 v(3\xi^2+10)/20 & h\xi^2v^2(9\xi^2+20)/120
\end{bmatrix}
$$

List of Figures